NTNU
Norwegian University of
Science and Technology

HYSYS Modelling of a Horizontal Three-Phase Subsea Separator

Rotimi Bayode Famisa

Chemical Engineering
Submission date: July 2016
Supervisor: Sigurd Skogestad, IKP

Norwegian University of Science and Technology
Department of Chemical Engineering

ABSTRACT

Subsea separators are very useful in the subsea for the separation of hydrocarbons and water. Its application has added value to the oil and gas industry as well as minimize the negative impacts of subsea operations on the environment. The objective of this thesis is to develop steady state and dynamic models of the three phase horizontal subsea separator in HYSYS. Then, comparatively investigate the separator model for optimization and control relative to a similar work by Tyvold.

Although HYSYS is based on "perfect" thermodynamic separation, it was possible to implement both steady state and dynamic models with non-ideal separators using the Real Separator capabilities of HYSYS. The HYSYS Real Separator capabilities offers the advantage of including carry over in order to match the separator design specification, and predicting the feed conditions or phase dispersion, device geometry, as well as inlet/exit devices on the carry over. The steady state model was optimized by performing simulations at different flow rates, oil cuts and residence time. The modelling approach was based on semi-empirical equations from stokes' law, GSPA as well as Barnea and Mizrahi correlations.

Several simulations were performed, on the HYSYS separator model, by varying the flow rates, oil cuts and residence time (factor) of the inlet stream: then, the separator efficiency was investigated by observing the purities of the product streams accordingly. Even though, the purities of the products did not meet the regulatory specification of 30ppm. This, probably, affirming the need for the integration of additional compact separator(s). Nonetheless, the model generally showed an acceptable response to changes in the input parameters compared to relevant theories in literatures.

Detailed information on three phase horizontal separator in HYYS are scare: nonetheless, useful data were employed from several literatures to implement this model. Data from the fields and experiments are required to further fit/improve on same. The Dynamic model particularly requires further fitting on the boundary conditions with data from the field or experiment.

Acknowledgement

I like to specially thank my supervisor, Professor Skogestad for his support and input. My appreciation also goes to Vlad Minasidis for his contribution and useful experience; to Tamal Das and Mohammad Ostadi for their valuable inputs. I acknowledge friends and colleagues for their helps. And my lovely wife for her valuable encouragements.

Table of Contents

List of Figures

List of Tables

Lists of Symbols

Symbol	Description	Unit
A	Cross section area	m^2
a_c	Centrifugal acceleration	ms^{-2}
α	Oil volume fraction / Oil cut	_
C	Concentration	$molm^{-3}$
D	Diffusion coefficient	m
D_d	Diameter of droplet	m2 s−1
F_d	Drag force	N
F_g	Gravitational force	N
FS	Flow split	–
g	Gravitational acceleration (≈ 9.81)	ms^{-2}
h	Vertical distance traveled by droplet	m
H_w	Height of weir	m
L	Length of separator	m
n_{dil}	Dilute efficiency	_
n_{dis}	Dispersed efficiency	_
p	Pressure	Pa
P	Density	kg/m^3
q	Volumetric flow rate	$m^3\ s^{-1}$
R	Radius of separator	m
r_d	Characteristic droplet radius	-
μ	Viscosity	Pas
V	Volume	m^3
v_X	Horizontal velocity	ms^{-1}
v_y	Vertical velocity	ms^{-1}
$Ø$	Diameter	mm

List of Subscripts/Superscripts

Acronyms	Description
b	Bottom product of gravity separator
C	Continuous phase
d	Droplet/dispersed phase
HPO	Heavy phase outlet
in	Feed/inlet stream to separator
max	Maximum
t	Top product of gravity separator
x	horizontal stream
y	Vertical stream

1 Introduction

Subsea processing has been around for some time now, but the recent growing confidence in the subsea separation has engendered huge research and investment with the objective of optimizing production and profit ultimately [41]. The immense advantages of the subsea production and processing has enabled viability from initially challenging reservoirs, which in consequence has enhanced oil production and recovery. This has also, economically prolonged the life of production fields. A major technology employed in deep sea processing is the separations of hydrocarbons and water using subsea separators. Subsea separators, in addition to processing hydrocarbon, also have capacity to handle water and sand at the seabed; and as such, reduces or stops the potential cost likely to be incurred from topside facilities. The use of subsea separator has greatly helped to minimizes environmental impacts and ensured a safer environmental process as against topside operations.

Subsea processing offers a flexible solution with a broad operating envelope for a wide range of operating conditions for gas-liquid fractions. It eliminates the use of risers, flowlines and topsides. It provides an effective and suitable resolution for flow assurance challenges, disuse topside facilities with limited production life (thereby foreclosing issues with operation cost and potential integrity) as well as transporting the fluids to other facilities with longer remaining life [10]. In this work, a three phase horizontal gravity separator will be modelled in HYSYS. The design approach of the horizontal separator is founded on semi-empirical equations derived from stokes law, GSPA as well as Barnea and Mizrahi correlations [22].

1.1 Objective

The subsea separator was modeled as a three phase horizontal gravity separator in Aspen HYSYS V8.6. The primary aim is to implement non ideal phase separation in HYSYS. Although HYSYS is based on “perfect” thermodynamic separation. But with the application of the correlation model setup in HYSYS, it was possible to remix the phases to real life situation by specifying the dispersions at the inlets and droplets sizes. Simulations were performed to investigate the performance of the separator.

1.2 Previous Work

This thesis is a continuation of my specialization project, Compact Subsea Separator Module of Oil-Water, in the fall of 2015. The project involved the study of different subsea separators and modeling of the horizontal gravity subsea separator of oil-water in HYSYS. And comparing the result to the thesis of Tyvold [33]. The Model implemented gave unexpected results, as such the need to continue the work in this thesis. The separator model has been modified and improved upon, in addition to reusing content from the specialization project.

1.3 Research Challenges

- Scare information on the HYSYS model especially for the dynamic state.
- Unavailability of field or experimental data.

2 Literature Review

2.1 Subsea Separation

Subsea processing involves the active treatment and handling of streams or fluids produced below the sea or at the seabed [13]. The processes primarily include:

- Pumping
- Gas/liquid separation
- Gas treatment as well as compression
- Water removal and disposal or reinjection
- Sand and solid separation

The decrease in bottom hole pressure following from the reduction in the wellhead backpressure, is considered a principal driving force in the application of subsea processing and production. This is helpful in boosting the production rate as well as ultimately increasing recovery [9]. Originally, the subsea processing was meant to alleviate the challenges during deep water production. But it is becoming extensively used for fields with damaging conditions to process equipment at water surface.

Subsea processing has several advantages of:

- Reduction in development costs
- Enriched recovery of hydrocarbons
- Enhanced flow rates
- A viable alternative and/or complement to chemical injection
- Reduction of environmental demages from occurrences of spills and leaks.
- Reduces personnel risks

2.2 Liquid-liquid Separation

Liquid-liquid separation involves the process of separating water and oil, and/or occasionally gas at the seabed. The technology was designed to extend the production life of mature fields by way

of high water cuts. But the use has become extensive in finding solution to developments with environmental and economic challenges. Removal of water from produced stream has the additional benefit of limiting the number and size of production pipes required for production, as such, safeguarding the equipment from the environment [32]. In Subsea liquid-liquid separation, there are three choices one can make regarding water produced from reservoirs [45]:

- Pump to the surface in separate flowlines
- Re-inject into the Reservoir or an adequate subsurface layer
- Expel into the sea

2.3 Reinjection of Subsea Water

The reinjection of Sea water is being widely used for support of reservoir pressure. It is important to note that the produced water is treated to the right quality before reinjection into the reservoir. Treated water usually contains traces of pollution from the residual oil as well as the production chemicals [6]. Treated seawater is primarily reinjected to support the reservoir pressure and secondarily to enhance recovery. The regulations established by the Petroleum Safety Authority Norway [32], requires the oil content in the water produced for discharge to be smaller than 30mg/l (30ppm). Although some industrial design (Troll Pilot and Tordis), specify otherwise that oil in water should not be more than 1000mg/l (1000ppm) [37].

2.4 Gains of Liquid-Liquid Separation

The goal of oil companies is to optimally produce hydrocarbons in the fastest, most economical and less costly ways. There are several benefits ensuing from subsea separation. Among these are the economical, operational as well as the environmental gains. The platform systems for fluid handling are usually limited, and this limited capacity can pose a problem for production because of the increasing water cuts resulting from an older field. The addition of a subsea separation unit to the field forecloses the need for the upgrade of the topside facility. Subsea separation provides the advantage of compacting process facilities on topside. The removal of water from the production stream results in reduction of the backpressure on the wells which in turn decreases the wellhead pressure. This wellhead pressure reduction increases the production rate from the well, as well as enhance the reservoir total recovery [33].

Subsea separation allows ease of accessibility to fields that were initially difficult to access due to their location at deep sea and the presence of heavy hydrocarbons. Subsea separation lessens the incidence of pollution from the platforms. The reinjection of water reduces or stops the discharge of water with oil residue into the sea [33]. Furthermore, the quantity of chemicals applied in the prevention of flow assurance complications are reduced, thereby reducing operational costs and environmental effect [21].

2.5 Challenges in Liquid-Liquid Separation

Subsea separation systems have limited accessibility, and consist of components that are prone to failure. Therefore, they should be easily retrievable in addition to providing alternatives that can be relied on [6]. The separator vessel is largely dominated with high pressure operating conditions at subsea. At great sea depths, the normal gravity separator design is usually too big and weighty because of the heavy thickness required to safe guard the device from the enormous hydrostatic pressure. The development of novel separator technology is now employed for this reason, typical examples are the pipe separator employed on Marlim and the semi-compact gravity separator assembled on Tordis [21]. Other challenges of the liquid-liquid separation in subsea, besides the separator, are regarding:

- Water handling and disposal
- Control of process system
- Sand handling method
- Sand and water quality measurement
- Flow assurance

Subsea separation of water comes with challenge of the disposal of the water. The existing options of injection into a disposal well, or into the production reservoir and disposal into the sea, all have limitations regarding the water quality. Therefore, an appropriate water processing unit need to be developed. In reinjection, the acceptable water quality is characterized by appraising the concentration, particulate sizes of oil droplets and particles in the water in which the limiting factors are the reservoir characteristics. Plugging and formation of filter cake can result from oil droplets and solid particles which accordingly weakens the reinjection process. [45]. The discharge

to the surrounding seawater is considered the simplest solution to the water separated saved for the tough environmental and legal regulations regarding the solids content residual oil and [42].

2.6 Theory of Separations

This chapter deals with the principles of separation, the applicable laws and equations used in the subsea horizontal separator.

2.6.1 Sedimentation

Sedimentation employs gravity in separating a liquid dispersed in the continuous phase of another liquid by using the difference in their densities. Consider a droplet having volume V_d and density ρ_d in a medium with density ρ, it will experience gravitational buoyancy force as in:

$$F_g = V_d(\rho_d - \rho)g \tag{2.1}$$

Where g is the gravitational acceleration, and can be substituted if the driving force is another factor other than gravity (e.g. centrifugal force). An object moving through a fluid experiences a frictional force, F_d as given by:

$$F_d = -\frac{1}{2}C_D A_d \rho |v| v \tag{2.2}$$

Where Ad is the reference area of the object, CD is the drag coefficient, and v is the relative velocity of the object with respect to the surrounding fluid. The drag coefficient is dependent on the relative velocity of the object to the surrounding fluid. Following from Stokes` law for laminar flow ($Re \ll 1$) the drag coefficient is given by:

$$C_D = \frac{24}{Re_d} \tag{2.3}$$

The droplet Reynolds number for a spherical droplet, Re_d, is given as;

$$Re_d = \frac{\rho v D_d}{\mu} \tag{2.4}$$

Where μ is the viscosity of the fluid and D_d is the droplet diameter and. The drag coefficient deviates from Stokes' law for an increasing droplet velocity within a flow regime of the transition region laminar and turbulent flow. A more appropriate expression for the drag coefficient in this

region is given by equation 2.5. This precludes the linear relationship between the drag force and the droplet velocity.

$$C_D = \frac{24}{Re_d}\left[1 + 0.1Re_d^{0.75}\right] \tag{2.5}$$

Conversely, for a valid Stokes' law (laminar flow around the particle), equations 2.1, 2.2, 2.3 and 2.4 are combined to give an explicit relationship for the terminal velocity of the droplet:

$$v = \frac{2r_d^2(\rho_d - \rho)g}{9\mu} \tag{2.6}$$

2.6.2 Viscosity of Emulsions

The relationship between the terminal velocity of a droplet in a gravity separator and the viscosity of the mixture is that of inversely proportionality (equation 2.6). The viscosity of an oil-water emulsion is dependent, plus other things, on the oil-water ratio and the droplet size of the dispersed phase [3, 44]. The viscosity reaches maximum at the point of phase inversion as shown in Figure 2.1.

Since the objective of the oil-water separator is to migrate the droplets from a continuous phase to another, they will have to move through the bulk interface. The composition closer to the bulk interphase will be close to the phase inversion composition (the mixture viscosity is high) and this in turn will reduce the separation rate.

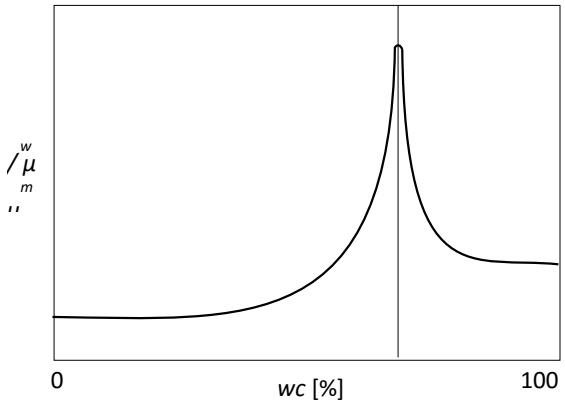

Figure 2.1: Qualitative illustration of the relative viscosity of an oil-water emulsion as a function of the water cut, wc. The relative viscosity is given by the ratio between the mixture viscosity, μ_m, and the viscosity of pure water, μ_w. The vertical-dashed-line is the phase inversion point. Arirachakaran [3], gave detailed and explicit illustration.

The viscosity of mixture is dependent on the tightness of the emulsion. The tightness of an emulsion describes qualitative the droplet sizes, with a tighter emulsion having smaller droplets than a loose one. The viscosity increases with the tightness of the emulsion and this in turn increases as the oil-water draws near the point of phase inversion [44]. This effect is described qualitatively for a water-in-oil emulsion in figure 2.2. The tightness (droplet sizes) of the emulsion entering a separator is, on the other hand, dependent on crude oil characteristics and the degree of turbulence it experienced upstream of the separator. The turbulence effect impacts the tightness, and thus the viscosity, which may trigger change in the emulsion as a function of the process variables (flow rates) in the separation system. This results in complications in predicting the separation rate.

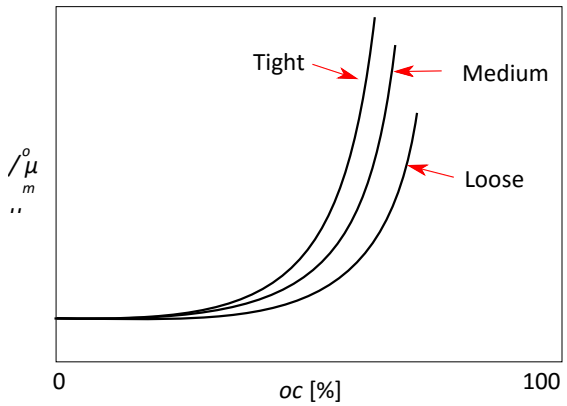

Figure 2.2: Qualitative illustration of the relative viscosity in a water-oil emulsion as a function of the oil cut, oc, for three emulsions with different tightness. See Woelflin [44], for detailed illustration.

Woelflin [44], concludes that the effect of the oil-water ratio on the mixture viscosity is large relative to the effect of the tightness. He also claims that, even with the several formulas for predicting the viscosity of emulsions, none of these is applicable over the wide range of the conditions in oil fields. If the effect of the emulsion tightness is neglected, equation 2.7 [34] can be used to define the mixture viscosity, μ_m, by fitting the coefficients of *a*, *b* and *c* to known data for a specified emulsion.

$$\mu_m = \mu_c \ \ 1 + a\varphi + b\varphi^2 + c\varphi^3) \tag{2.7}$$

Where ϕ is the dispersed phase volume fraction and μ_c is the viscosity of the continuous phase.

2.7 Diffusion

The gravitational sedimentation forces trigger the separation process in the separator, and as a result there is concentration gradients in the direction of separation. This also will lead to diffusion by Brownian motions, with an opposing effect on the separation. The diffusion in an emulsion having a concentration gradient in the x-direction is defined by Fick's 2. law [29];

$$\frac{dC(t,x)}{dt} = D\frac{\partial^2 C(t,x)}{\partial x^2} \tag{2.8}$$

Where $C(t,x)$ is the concentration of the dispersed phase and D is the diffusion constant for the given system

2.8 Coalescence

Coalescence occurs when two droplets fused together into one in a separator as seen in Figure 2.3a, and also when droplets fuse with the continuous phase via the bulk interface, see Figure 2.3b. The first phenomenon results from the different velocities of the droplets caused by their velocities of sedimentation, turbulence, diffusion and the rest. This intensify collisions thereby causing the droplets to coalesce as a function of the attractive and repulsive forces between the droplet as well as their kinetic energies. Coalescence speeds up separation following from the growth of the droplets engendered by sedimentation. Droplets coalescence through bulk interface is essential in separation theory for separation of droplets from the surrounding phase. In instances of high interfacial tension, this process becomes rate determining while the droplets accumulate closely to the bulk interface.

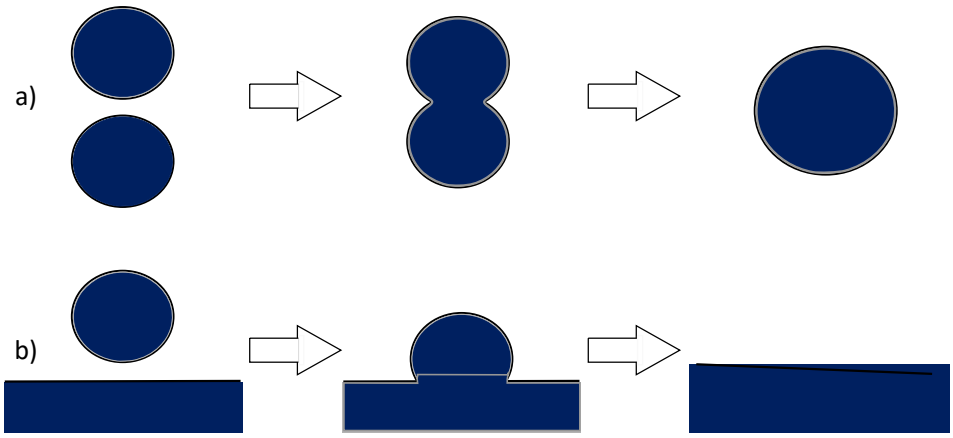

Figure 2.3: a) Two droplets coalesce to form one bigger droplet. b) A droplet coalesces with the bulk phase.

2.9 Separation Efficiency

In Liquid-liquid separation, it is very important that the product streams meet the regulatory product specification. Water entrained in oil is capable of affecting the quality of product, therefore, there is need for further effluent treatment to separate the entrained oil. The oil and water products specifications are set by environmental regulators. The performance of a separator is often defined by its separation efficiencies. Some of the commonly used methods are the dilute or dispersed efficiencies given in equations 2.9 and 2.10. Depending on the feed specification, a designer can employ different approaches to meet the required separation. See the sub section for further discussions on the different approaches of defining oil-water separation and as well as its effect on final design.

$$\eta_{dil} = \frac{\alpha_{LPO} q_{LPO}}{\alpha_{in} q_{in}} \qquad (2.9)$$

$$\eta_{dis} = 1 - \frac{(1 - \alpha_{LPO}) q_{LPO} + \alpha_{HPO} q_{HPO}}{q_{in}} \qquad (2.10)$$

Where η_{dil} and η_{dis} are the dilute and dispersed efficiencies, respectively. While q_i and α_i are the volumetric flow rate as well as the oil volume fraction of stream *i*, respectively.

2.9.1 Droplet distribution

A supposed perfect method of defining the separator feed will be to count the number of droplets in diverse sizes in lab and plot distribution curve. Figure 2.4, Curve-A is a characteristic curve that typifies droplet volume percent against droplet size. It is important to note that the droplet size distribution is not basically a normal distribution as in the figure. Droplet volume fraction may take any shape or be ascending or descending, based on the droplet formation mechanism, system configuration and physical properties of the liquids. Different range of droplet size and their fraction can exist. For example, mechanical processes (like pumping, mixing and transporting two phase flow) produce much larger droplet sizes than the chemical reactions.

Curve B is produced from curve A with the cumulative droplet concentration shown. This curve is useful in helping a designer to select the optimized separation technology in addition to guaranteeing equipment performance. With this Curve, process designer can now determine if it possible to achieve the desired separation level, with or without internal device, with gravity separation. The gravity separation of very fine droplets results in unreasonable enormous sizes.

A typical example is observed from Figure 2.4 (with water fraction of 1.4 vol% in oil), reduction of the water content level to 0.2 vol% (200ppmv) requires separating droplets of roughly 100 microns and above. This is the customary practical size for separation with gravity when the difference in the density of the phases is small and/or a lower viscosity of the continuous phase.

To achieve further reduction in water, carry over, an internal device having separation efficiency as in Figure 2.5 is considered a suitable selection. The device is capable of improving gravity settling as well as separating particles from 40 microns and above. The cut-off diameter is 40 microns. From Figure 2.5, smaller particles than 40 microns are separated at lower efficiencies. With this specific internal, we would also have a new droplet distribution for the separator outlet as in Figure 2.6, typifying 0.025 vol% (250 ppmv) of water content in the oil product from the separator. It is important to note that the oil droplets distribution in water as well as the internal device removal efficiency for oil droplets may not be same as that of water droplets [47].

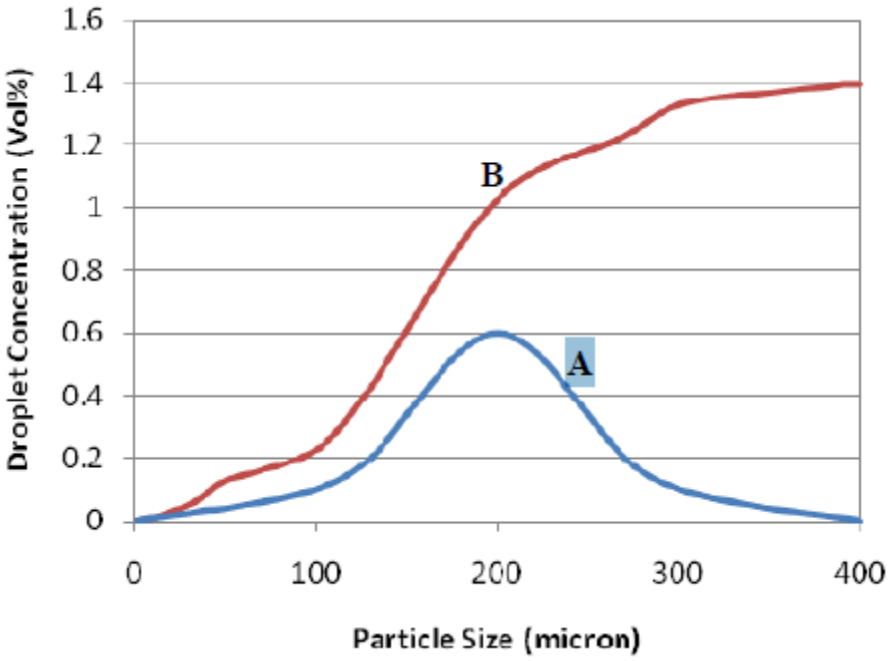

Figure 2.4: Water droplet distribution at separator inlet [47]

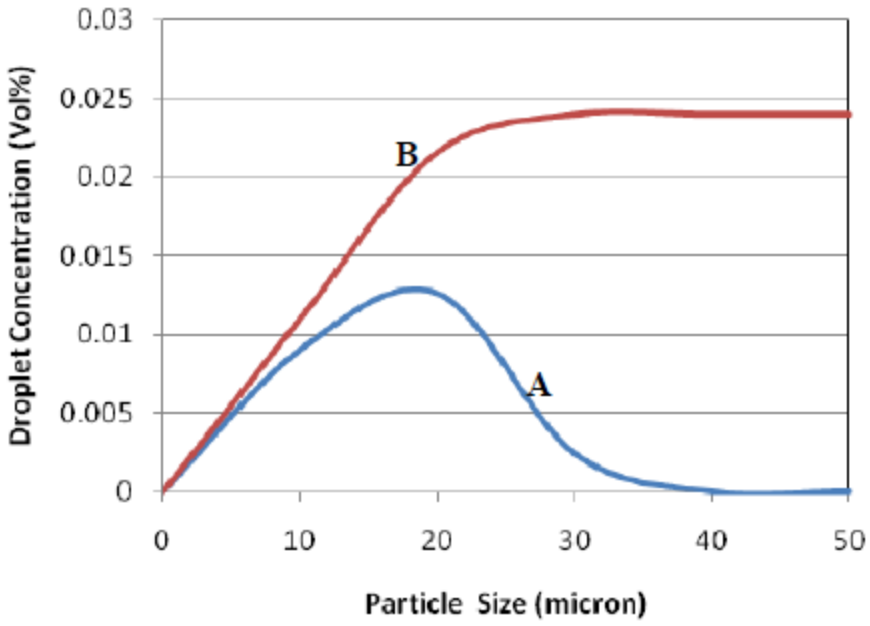

Figure 2.5: Water droplet distribution at separator outlet [47]

2.9.2 Residence time

Laboratory techniques might be useful to define the characteristics of feed separation with direct measurement of the required time for the oil and water to separate out. In this approach, the residence time of the phases or the entire separator is estimated from the observation of the laboratory tube. While the result from this approach is obtained from laboratory test, nonetheless, it requires real plant demonstration to ensure the required separation is achieved. This residence time is only reliable if the outcome is gotten from repeated sampling of oil and water phases to confirm the contamination level. This approach of feed specification and separation requirement is useful for gravity separation. However, if internal device is necessary, the prediction of its effect on final separation is difficult [47].

For residence time with similar experience with the same fluid in existing fields, care must be observed to integrate it into design because the parameters of design change during plant life (particularly for production plants). This approach will be invalid for new design using technology different from existing one.

Some Clients make reference to API-12J, specification for oil and gas separators, in which typical residence time has been specified for various type of oil (as shown Table 2.1). This method has the disadvantage of not customizing based on actual characteristics of the feed **[**47**].**

It is important to state that none of these methods can guarantee the meeting of the product specification except extra measures are taken by the designer of the equipment in ensuring the equipment performance.

Oil API Gravities	Separation Temperature (°F)	Residence Time (min)
> 35°	Any	3-5
< 35°	> 100	5-10
	> 80	10-20
	> 60	20-30

Table 2.1: API Recommendation on residence time [47].

2.9.3 Cut-off diameter

There are a lot of projects where none of the above mentioned methods can be used to specify the required liquid-liquid separation. That is, the separator outlet is stated for the project but no adequate definition of the separator feed. Instances like this require the assumption of an appropriate droplet distribution curve in which a cut-off diameter at which the desired separation is attained is adopted. In order to product such graph, s minimum of three points are needed; maximum droplet size (dmax), mass mean droplet size (d50) and Sauter mean droplet size (d32). Furthermore, the provision of these data requires laboratory screening of the droplets which is infeasible in design stage. As such, the use of cut-off diameter basis for sizing the separator is recommended. The relationship between a given cut-off diameter and the specification of the separator outlet is shown in Figure 2.6. The graph can be employed for designing oil and water (production) separators as well as similar applications having the particles droplet within the same range. This figure is not applicable to processes with very small droplets generated or with a relatively different shape of droplet distribution curve from figure 2.4.

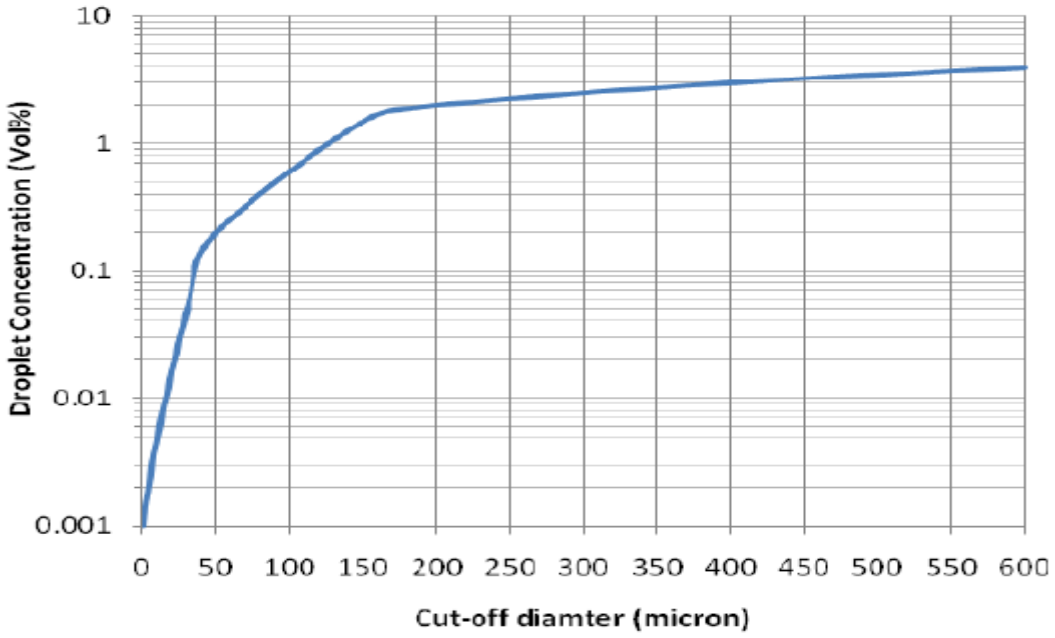

Figure 2.6: Droplet carry over vs. cut-off diameter [47]

2.10 Rossin-Rammler

There is need for characterization of particles using their size measurements. This is useful in the proper analyses of particle size distribution in a given system. But if the needed data are not readily available, reference can be made to known characteristic values for the system. Particles size distribution are expressed as continuous mathematical functions like Gaussian and Rossin-Ramler or as discrete statistics. These mathematical functions use two parameters of central tendency and spread. It is important to state that the application of continuous distribution functions to denote experimental data is a compromise, this is because measured data hardly fits the model accordingly. Nonetheless, the advantage of the distribution functions making it possible to compare large data with some limited basic parameters.

Rossin-Rammler is mathematically defined by:

$$F = exp(-d/dm)_x \tag{2.11}$$

Where*: F* is the total of droplets volume fraction larger than *d, dm* is related to *d95, x* is the RR index, *d95* is 95% of droplets smaller in size than this diameter for the specified dispersion, *RR Index* is the spread parameter exponent applied in the *RR* equation (also known as the "spread parameter*")* * mode is the frequently occurring diameter (i.e. peak of the frequency curve/histogram), compared to the other several measures of central tendency like the mean or median diameters.

** spread is a measure of degree of deviation away from the central tendency; its value is typical of the system/substance considered. It can otherwise be defined as:

$$\ln(F) = (-d/dm)_x$$

or

$$\ln(1/F) = B + x ln(d) \tag{2.12}$$

Where, *B* is a constant given as *ln (1/dm)*

Hence, the plot of ln(ln(1/F) against ln(d) is used to evaluate the *R-R* parameters. If the plot is not a straight line, it means the particle distribution cannot be sufficiently described by the Rossin-Rammler function. The HYSYS Real Separator correlations uses the *d95* data other than dm. Where, *dm* is calculated from *d95* as in equation 2.13

$$dm = d95/\left(-ln(1-0.95)\right)^{1/x} \quad (2.13)$$

3 Model Description

The following sections describe the model of the horizontal gravity separator and the main assumptions made in this context. This includes the horizontal and vertical velocities, the droplet sizes and the viscosity in the separator, parameters used in the design of the model, correlations and methodologies applied. A summary of the model is presented in section 3.8

3.1 Description of HYSYS Modeling Tool

The essence of utilizing HYSYS simulation is to get a broad understanding of the process. It also allows one to know how changes influences the process variables of product composition, temperatures and pressures [18]. The steady state and dynamic modeling tools are useful in the design and optimization of chemical processes. Steady state model is used to maintain the material and energy balances while evaluating different plant scenarios. It is mostly utilized in optimizing the process through cost reduction and maximizing production. The dynamic model is important in confirming whether the desired results are being produced in addition to safety concerns and ease of operation of the production. This is usually used in the optimization of controller design and to get information regarding the conditions of startup and shutdown. Balances derived from the dynamic model are similar to that of steady state, save for the inclusion of accumulation term. The accumulation term specifies the changes in the output variables with time [2]. Typical devices used in the industry have material inventory (holdup). In such instances, the dynamic modeling tool is helpful.

The software is also widely employed in chemical engineering industry, researches, modeling, development, and design [18]. HYSYS provides the platform for the creation of both steady state and dynamic simulations, and evaluate the model from either of the two perspectives. The modeling tool is furnished with various operations plus designs that enables simulations of different processes. HYSYS can also model upstream, gas processing, chemical and refining processes from the [18]. During model development in HYSYS, it is essential to use the appropriate fluid package and specific components. The Simulation Basis Manager (SBM) allows for the selection, addition and modifications of fluid packages, reactions and components. If one

is uncertain regarding the choice of fluid package, useful recommendations can be obtained from the Property Wizard. It is only important to specify two of the parameters of pressure, temperature and vapor fraction, plus the mass/molar flow rate as well as the composition. HYSYS will automatically generate the remaining parameters for both downstream and upstream.

3.2 Modeling Separators in HYSYS

The Separator operations in HYSYS is based on "perfect" thermodynamic separation. But in real world, separation is not perfect; because the different phases of the liquids and gas can be entrained in one another. Over the years, vessel internals (weirs, mesh pads, vane packs) are increasingly used to limit carry over of entrained gases or liquids. But with the HYSYS Real Separator capabilities, non-ideal separation can be modeled in steady and dynamic states. The real separator offers the advantage of: first, including carry over in order to match the separator design specification/process mass balance, and second, predicting the feed conditions/phase dispersion, device geometry, as well as inlet/exit devices on the carry over [25,48].

3.3 Carry Over Models/Options

This model allows for the liquid and gas carry over to be calculated or specified. It is used to model non-ideal separation in steady and dynamic states. Three types of correlations are currently available for the real separator capabilities of the carry over option in HYSYS V8.6. They are the feed basis option, the product basis option and the Correlations option or Model. Since the ideal separator assumes perfect separation based on thermodynamic equilibrium calculations (Carry Over Model is checked to None). The vessel pressure drop is taken as negligible compare to the nozzle pressure drop and as such fixed to zero [25,48]. The carry over option/models can be one of the following discussed in subsequent subsections.

3.3.1 Feed Basis Model

In this model, one can easily specify the carry-over of the individual phase in the product outlets as a fraction or percentage of the feed. For non-zero specification, the product outlets from the device will contain multiple gas and liquid phases. Two checkboxes are available for use on the Feed Basis page: First, “carry over to zero flow streams”, which allows for a specified carry over into the product stream nonetheless there is no flow. Second, “the checkbox of Use PH flash for product streams”, this make active the HYSYS flash from PT to PH for the product streams. This is only used when there are issues with inconsistencies in the PT flash. These checkboxes are similarly obtainable for use in the Product Basis as well as the Correlation Based models [25,48].

3.3.2 Product Basis Model

The model allows us to specify the carry over in the product outlets in mass/mole/volume flow or fraction. In the event of one phase missing in the feed stream, ticking the “Use 0.0 as product spec if phase feed flow is zero”, makes it possible for the separating device to calculate the effect of the carry over (by ignoring any flow specification or product fraction for that phase). The feed and Product models both have six types of carry over flow (in their feed and product streams) available for specification, they are namely: Light liquid in gas; Heavy liquid in gas; Gas in light liquid; Heavy liquid in light liquid; Gas in heavy liquid; Light liquid in heavy liquid [25,48].

3.3.3 Correlation Based Model

Here, the expected carry over is calculated following from the feed conditions, the design of the vessel and the type of the inlet/exit devices fitted in the separator. The necessary information can be readily fed in on the Dimensions Setup, Correlation Setup and the Nozzle/DP Setup pages. With the Correlation Setup, it is possible to choose a Correlation calculation type and how it should be applied. One can apply a single correlation for the calculations of carry over by selecting the “Overall Correlation radio button”. Otherwise, choice of correlation for each step can be made from the carry over calculation sequence.

3.4 Correlations Details

The carry over can be calculated from three different correlations: Generic, ProSeparator, and Horizontal Vessel. Each of the correlation is furnished with a “view Correlation” button to see its parameters.

3.4.1 Generic Correlation

The Generic correlation uses a general method for the estimation of the phase dispersion in the feed as well as for defining the separation basis. This generic calculation ignores vessel configuration. The user specifies the fraction of each feed dispersed in each other feed phase and the Rossin-Rammler parameters (Rossin-Rammler index and d95 droplet size) for the individual dispersion. The distributions of the inlet droplet of the dispersed phase are then calculated from these specifications as discussed in section 2.10. The calculation of the carry over is done based on the assumption that droplets smaller than a certain critical droplet size are all carried over [25,48].

3.4.2 Horizontal Vessel Correlations

These correlations were developed for the horizontal three phase separator. The Horizontal Vessel correlations use a defined” Inlet Hold up” (user-specified dispersion fractions), and an assumed efficiency of the inlet device to calculate the six different types of dispersions in the feed. These parameters can be accessed on the Setup via General page of the Horizontal Vessel Correlations view). A user-specified Rosin-Rammler parameters were used to calculated the droplets distribution of the dispersed phases. Then, the liquid-liquid dispersion droplet d95 is calculated from the densities of the two liquid phases and the inlet droplet d95.

The primary gas-liquid separation is estimated by using the residence time of the gas in the device and the settling velocities of the light and heavy droplets in the gas phase. A droplet is entrained if the vertical distance needed to rejoin its bulk phase is greater than the vertical distance it travels during its residence time in the separator. The primary liquid-liquid separation is also calculated with the settling velocities for each liquid droplet or gas in the liquid phases in addition to each

liquid phase residence time. The GPSA correlations are used to calculate the settling velocities for all dispersions, however, Barnea and Mizrahi method is used for calculating the settling velocities for the water in oil dispersion. The correct liquid phase viscosities (i.e. water-in-oil and oil-in-water) are calculated by a user-defined liquid phase inversion point. One can also apply a residence time correction factor. "A droplet is carried over if the vertical distance traveled during its residence in the vessel is less than the vertical distance required to rejoin its bulk phase" [25,48].

3.5 GPSA Correlations for Dispersions (Settling Velocities) or Gravity Settling

According to the Gas Processors Suppliers Association (GPSA) [16], liquid droplets drop out of a gas phase when the force of gravity on the droplet is more than the drag force of the gas moving around the droplet as seen from figure. 3.1. The mathematical description of these forces are given in equation 3.1

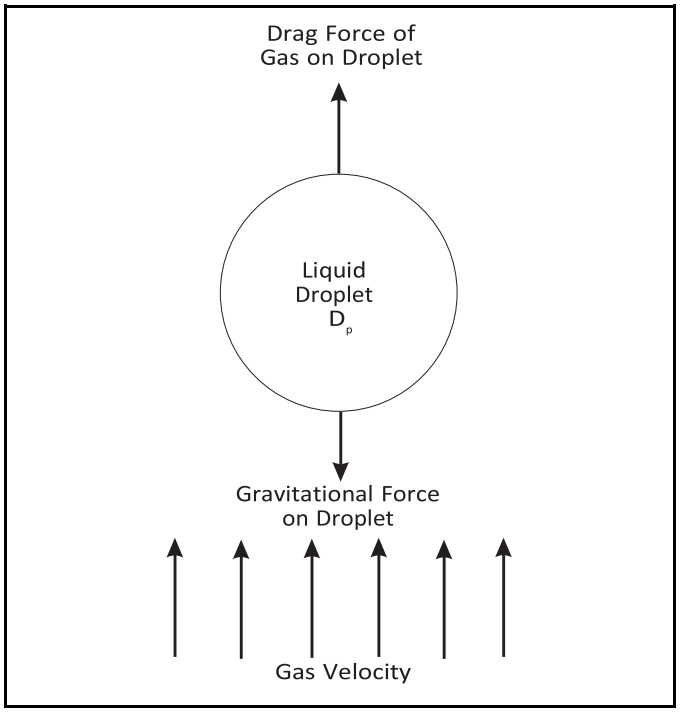

Figure 3.1: Forces acting on Liquid Droplet in Gas Stream

$$V_t = \sqrt{\frac{2gM_P(\rho_l - \rho_g)}{\rho_l \rho_g A_p C'}} = \sqrt{\frac{4gD_P(\rho_l - \rho_g)}{3\rho_g C''}} \tag{3.1}$$

where V_t is the critical or terminal gas velocity required of the particle size D_P, M_P is the mass of the droplet/particle, ρ_l is the liquid phase density, droplet or particle, ρ_g is the phase density, A_p is the particle/droplet cross sectional area, D_P is the droplet diameter, g is acceleration due to gravity, and C' is the drag coefficient of the particle.

The drag coefficient is a function of the Reynolds number and the particle shape of the flowing gas. In this case, the shape of the particle is assumed as a solid rigid shape. Therefore, the Reynolds number is given as:

$$Re = \frac{1{,}488 D_p V_t \rho_g}{\mu} \tag{3.2}$$

The relationship between the Reynold number of a spherical droplets and the drag coefficient is shown in figure 3.2

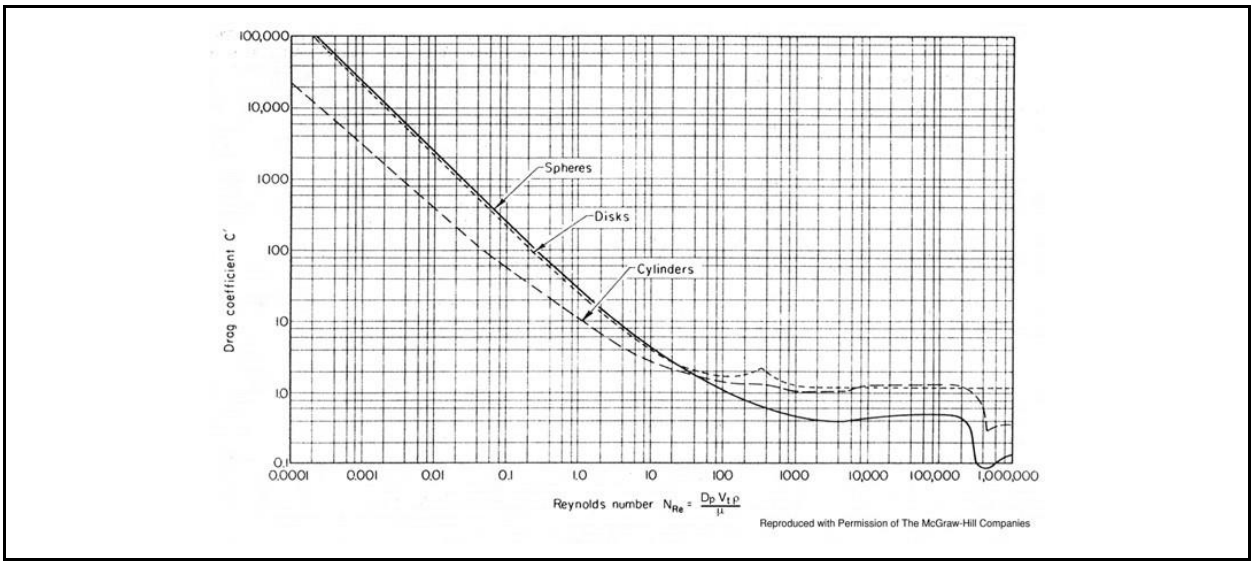

Figure 3.2: Reynolds Number and Drag Coefficient for Spherical Particles [16.]

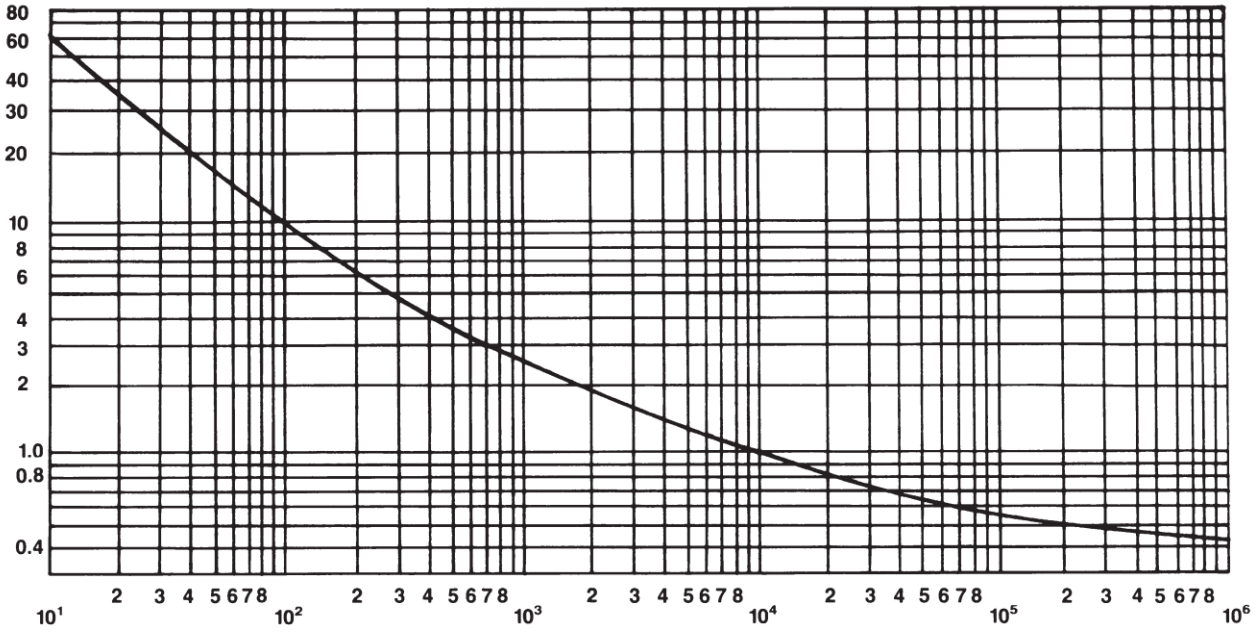

Figure 3.3: Drag Coefficient for Rigid Spheres [17]

A trial and error solution is needed for this form, because both the terminal velocity and particle size are involved. But in order to avoid this approach, the drag coefficient is then represented in figure 3.3 as a function of the product of the square of the Reynold number times the drag coefficient. This approach eliminates velocity from the equation [16]. Therefore, the abscissa of figure 3.3 is defined by:

$$C'(Re)^2 = \frac{(0.95)(10^8)\rho_g D_P^3(\rho_l - \rho_g)}{\mu^2} \tag{3.3}$$

At high Reynolds number, the drag coefficient of gravity settling of other fluid flow phenomena attains a limiting value. Another alternative to the use of equation 3.3 and figure. 3.3, is simplifying the curve in Fig. X1 into three divisions from where one derives a C' vs Re curve-fit approximation. Substituting these relationships into equation 3.1 gives three settling laws explained in subsection below.

3.5.1 Stoke`s Law

For Reynolds numbers less than 2, there exist a linear relationship between the Reynolds number and the drag coefficient (laminar flow). Since Stoke`s law is valid, equation 3.1 is defined as:

$$V_t = \frac{1{,}488\ g\ D_p^2(\rho_l - \rho_g)}{18\mu} \tag{3.4}$$

The droplet diameter for a Reynolds number of 2 can be calculated by using 0.025 for K_{CR} in equation 3.5

$$D_P = K_{CR}\left[\frac{\mu^2}{g\ \mu_g(\rho_l - \rho_g)}\right]^{0.33} \tag{3.5}$$

Fig. X4 shows the summary of these equation, in addition to the general information concerning the sizes of the droplet as well as the selection guidelines for the collection equipment.

3.5.2 Intermediate Law

The Intermediate Law applies for Reynold`s numbers between 2 and 500, therefore, the terminal settling law can be defined as:

$$V_t = \frac{3.49\ g^{0.71} D_P^{1.14}(\rho_l - \rho_g)^{0.71}}{\rho_g^{0.29}\mu^{0.43}} \tag{3.6}$$

The droplet diameter at a Reynolds number of 500 is found by using 0.334 for K_{CR} in equation 3.5 This law is valid for several of the liquid-liquid and gas-liquid droplet settling phenomena in gas processes.

3.5.3 Newton`s Law

Newton Law is valid for Reynold`s number between 500 – 200,000, and applied widely in separation of big particles/droplets from a gas phase. The drag coefficient is about 0.44 for Reynold`s numbers above 500. Putting the value of C' = 0.44 into equation3.1 redefines the Newton`s Law as:

$$V_t = 1.74 \sqrt{\frac{g\ D_P(\rho_l - \rho_g)}{\rho_g}} \tag{3.7}$$

Reynold`s number upper limit is 200,000 and $K_{CR}$ is 18.13 at the Newton`s Law region.

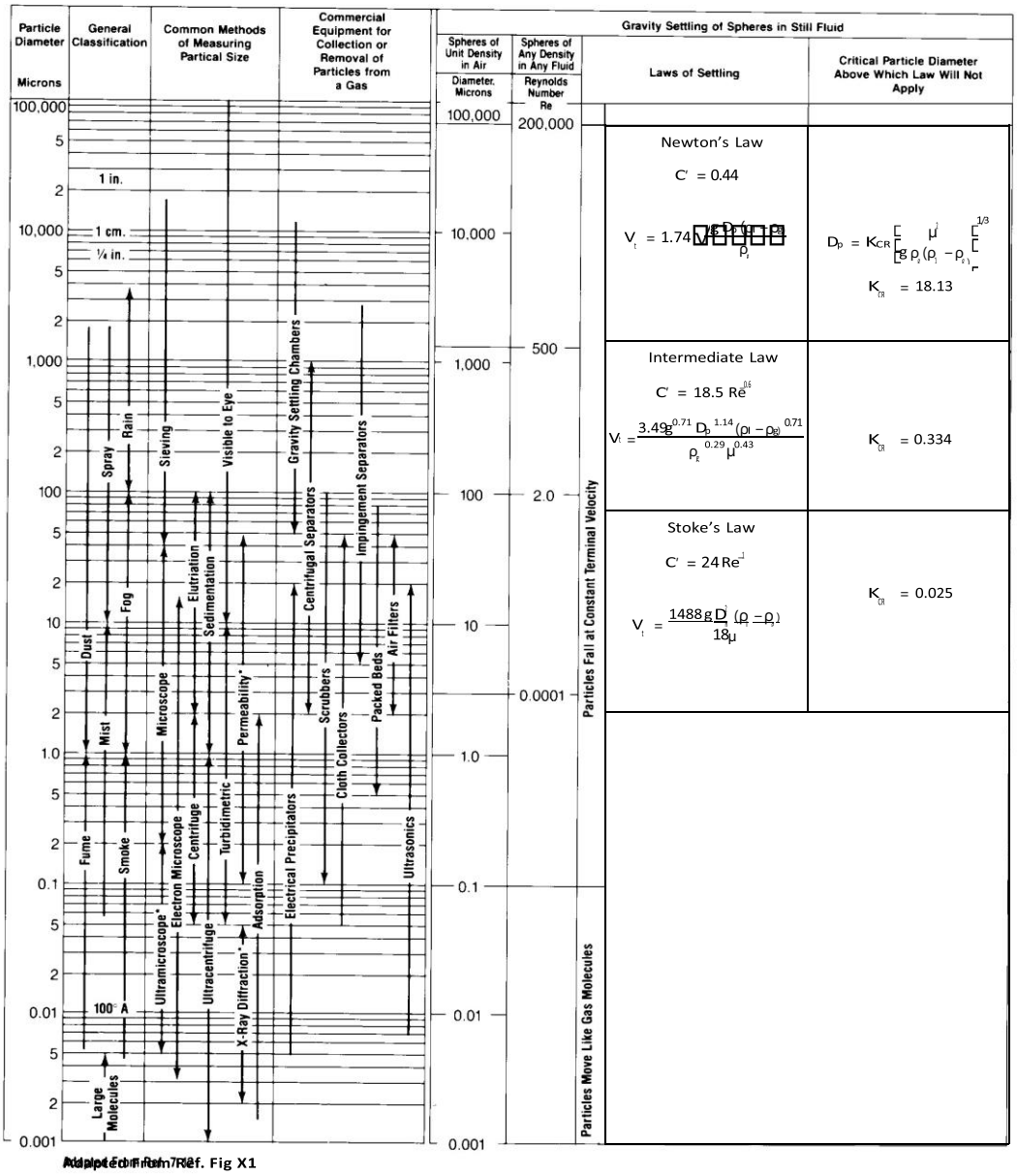

Adapted From Ref. Fig X1

Figure 3.4: Gravity Settling Laws and Particle Characteristics [17]

3.6 Barnea and Mizrahi Method of Correlation for Gravity settling

According to Barnea and Mizrahi [5], the relative velocity between a continuous fluid medium and a multi-particle cloud is a function of the volumetric concentration and the size of the particles, considering the system physical parameters. A new general correlation was developed to organize and unify the different published data from experimental in this field, thereby providing a dependable reliable design method. The design covers solid particles as well as correlation regarding liquid drops in fluid medium; and further applied to fluid flow through fixed particles systems.

3.6.1 Basic Assumptions

i. This approach deals with spherical particles systems, having similar specific gravity, a relative narrow size distribution which can be reduced to average characteristics size. This model might be extended in the future to the effect different kinds of particles or particle shape factors.

ii. Except for the fluid hydrodynamic effects, no any kind of interactions exist between the particles.

iii. The particles positions in the cloud are completely and relatively random, without any segregation. In real life, the size segregation effects become greater with a larger size distribution span. The increase of the particles` volumetric concetration counters these effects. Heavily populated clouds enhance their homogeneity with the help of their internal filtration capability. Thereby bringing closer to reality the assumption of random order, with more concetrated suspensions and narrow size distributions.

iv. Neglect the container walls effect; this valid for several industrial equipment but some what delicate in evalution of experiments on laboratory scale.

3.6.2 Gravity Settling of a Single Particle

The various physical parameters (fluid density ρ_c, fluid viscosity μ_c, the particle density $\rho_{d,}$ and the gravitational acceleration g) in addition to the variables of the particle diameter d and its relative

velocity *U*, are classified according to the principle of similarity, into two dimensionless groups represented as coordinates in figure 3.5.

$$Re = \frac{Ud\rho_c}{\mu_c} \tag{3.8}$$

$$C_D = \frac{F_D}{\frac{1}{2}\rho_c S U^2} = \frac{(\prod/6)d^3(\rho_d - \rho_c)g}{\frac{1}{2}\rho_c S U^2} \tag{3.9}$$

Where S is the largest cross sectional area of the particle given as $\prod d^2/4$ for sphere. Figure 3.5 permits the linking of the two variables through the method of trial and error.

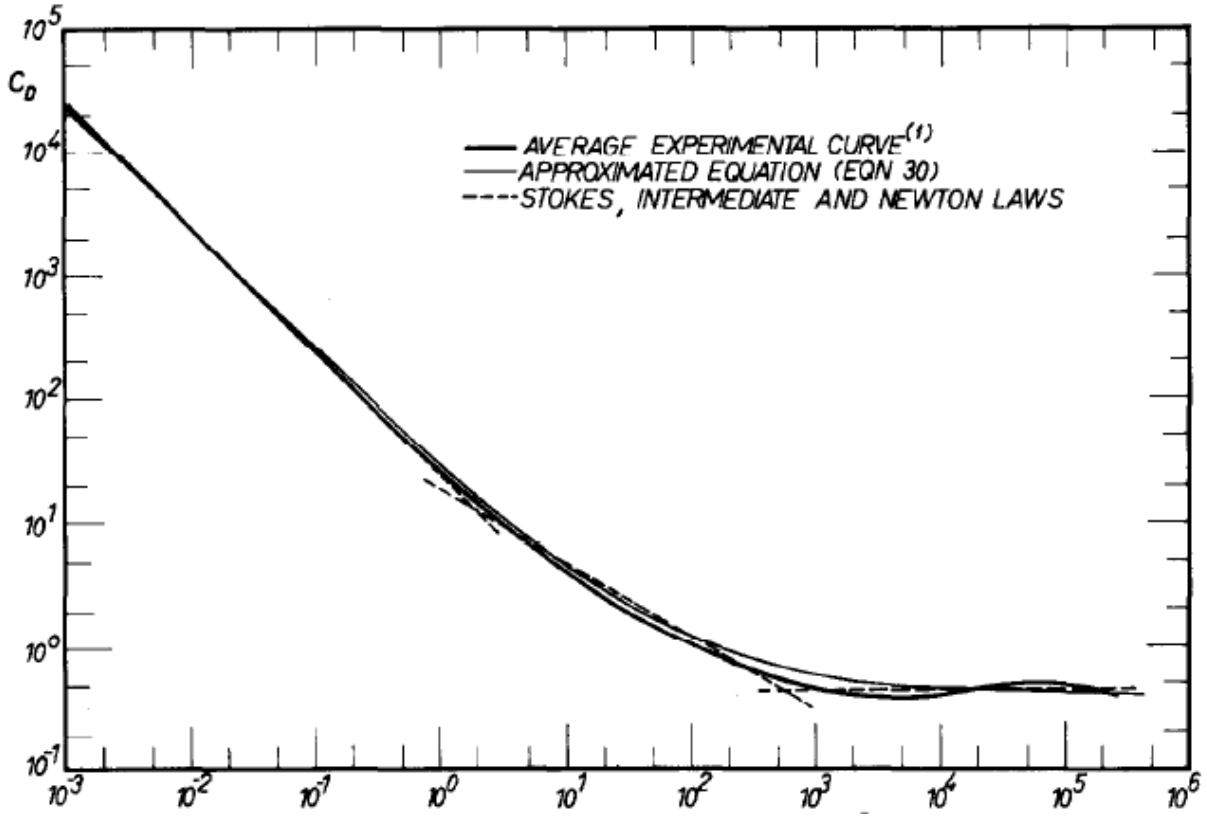

Figure 3.5: Correlation of the drag coefficient vs. Re for a single solid [5]

3.7 Process Description

The input to the data is two streams of oil and water as shown in figure 3.6. The input parameters of the streams in Tables 3.1 and 3.2, were adopted from different sources [11,23].

The two streams were mixed in the Mixer before entering the three-phase separator. The separate streams of the oil and water before the Mixer allows for the variation of the oil cut of the Mixed stream. The weir-type horizontal subsea separator was adopted as the basis for this design. There are three units within the separator: the initial separation unit, the gravity settling unit and the end unit, as seen from figure 3.7. The streams of the oil and water jointly enter the vessel from the initial separation section. A mounted cyclone absorbs the streams momentum and further directs the liquid to the bottom and the gas to the top of the device. The fluids go through perforated baffle plates into the gravity settling unit. The baffle plate improves the fluid linear momentum along longitudinal axis. At the inlet of the settling unit, we have various phases containing distributions of oil droplets, water droplets and gas bubbles (assumed as 10% for this work). These droplets and bubbles are separated when they travel to their different continuous phases. The end section consists of the outlets nozzles, a weir and a vane demister. The weir helps to improve the separation efficiency between the heavy and light liquids. The oil and water nozzles are incorporated with vortex breakers. The vane demister, mounted before the gas outlet nozzles, removes tiny droplets of liquid.

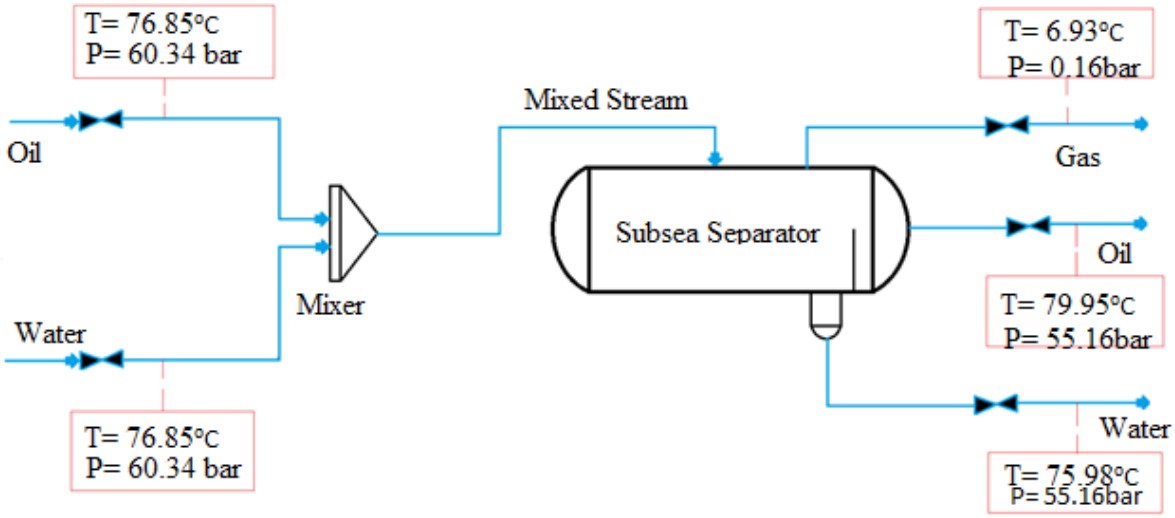

Figure 3.6: *Flowsheet of the model with some parameters*

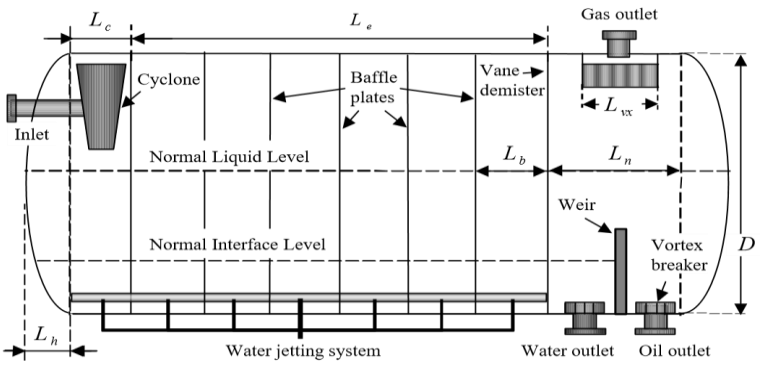

Figure 3.7: Three-Phase horizontal separator (Weir type)

Figure 3.8, further shows how the gravitational buoyancy forces push the dispersed oil droplets upward and the continuous water phase downward. This leads to the continuous oil phase being formed at the top of the separator and a pure water phase settling at the bottom. The vertical weir at the end of the separator separates the flow into two streams of top (q_t) and bottom (q_b) products. The top product, q_t is collected behind the weir while the bottom product, q_b exits below the weir. The top location of the separator behind the weir, allows for the removal of gas from the vessel. Some of the input parameters to the HYSYS model were obtained from an optimal design model of a similar three phase horizontal separator of oil-water [11]. The steady and dynamic states model were implemented, both models are located in Appendixes **B.1** and **B.2**, respectively.

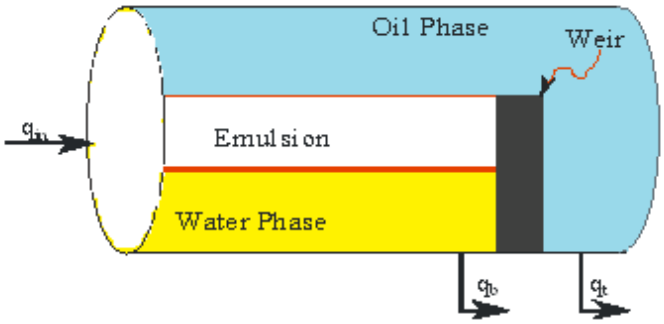

Figure 3.8: Horizontal gravity separator. The liquid is fed into the separator as an oil-in-water emulsion. As the gravitational buoyancy forces push the oil droplets upward, a continuous oil phase is formed in the top of the separator and a pure water phase settles

3.8 Horizontal Three Phase Subsea Separator

The subsea separator was modelled as a three phase horizontal gravity separator in Aspen HYSYS V8.6. Although HYSYS is based on "perfect" separation; nonetheless, the separator was modelled closely to what is obtainable in real life. This was possible by using the Real Separator capabilities in which the Carry Over Option was employed because of the advantage of allowing for the specification of the various dispersion accordingly. In addition, the model is correlation based since it allows for the specification of the three phase horizontal vessel correlation. The Rosin-Rammler parameters were used to calculate the droplets distribution of the dispersed phases. Liquid-liquid dispersion droplet d95 was calculated from the densities of the two fluids of oil and water. The primary gas-liquid separation was estimated by the residence of the gas in the vessel in addition to the settling velocities of the oil and water droplets in the gas phase. Primary liquid-liquid separation was calculated by each liquid droplet settling velocities or gas in liquid phases and the residence time of each liquid phase. The HYSYS model used Barnea and Mizrahi method [5], to calculate the settling velocities of the water in oil dispersion while GPSA correlation [15], was also utilized for the calculation of other dispersions. Detailed description is in sections 3.5 and 3.6. The fluid package for the model is Kabadi Danner, which is the recommended package for hydrocarbons with water solubility [24]. The basic HYSYS model files are located in Appendix **B**.

3.8.1 Horizontal Velocity

The flow through the separator is modeled as two separate plug flows separated by the height of the weir (H_w), as seen from figure 3.9. It is assumed that there is no net mass transfer between the plug flows, but oil droplets will rise from the bottom part to the upper part with equal volumes of water moving in the opposite direction. The liquid hitting the weir at the end of the separator is supposed to exit through the bottom outlet, while the liquid above H_w is assumed to flow over the weir and exit through the top outlet.

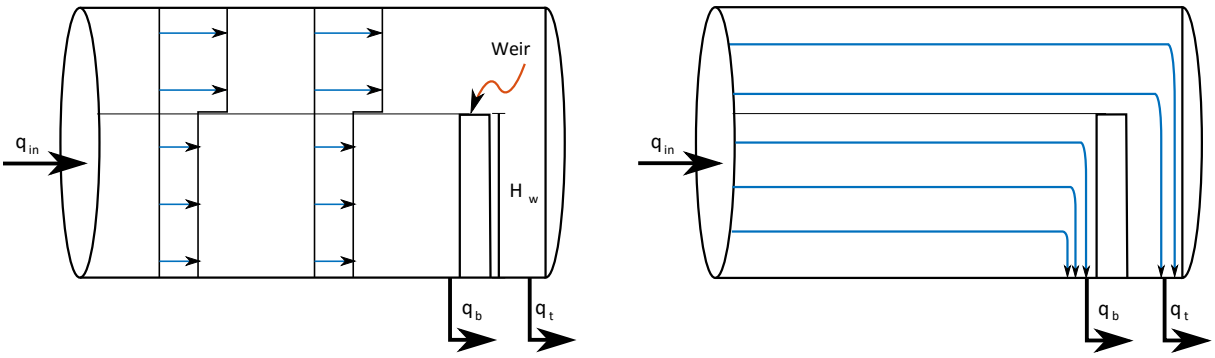

(a) Horizontal velocity profile. (b) Stream lines.

Figure 3.9: The horizontal flow model in the gravity separator is divided into two regions. The liquid under the weir is assumed to have a constant horizontal velocity until it hits the weir and exits through the bottom outlet (qb). The liquid over the weir also h

The valves on either of the outlet streams are used to manipulate the flow rates of the two plug flows, by adjusting the horizontal velocity, v_x, of the droplet moving through the separator under H_w. And it is assumed to be equal to that of the continuous phase which is given by;

$$v_x = \frac{q_b}{A_b} \tag{3.10}$$

where A_b is the cross section area of the circular segment limited by H_w (lower part of the separator) and q_b is the volumetric flow rate of the bottom outlet product. The cross section area is derived from simple trigonometry as;

$$A_b = \frac{R^2}{2}\left[2\cos^{-1}\left(\frac{R-H_w}{R}\right) - \sin\left(2\cos^{-1}\left(\frac{R-H_w}{R}\right)\right)\right] \tag{3.11}$$

Where, R is the radius of the separator.

3.8.2 Vertical Velocity

The vertical velocities of the droplets are triggered by the gravitational buoyancy forces and they are given by equation 2.6 with the assumptions discussed in Chapter 2.1. Equation 2.6 is restated below.

$$v_y = \frac{2r_d^2(\rho_d - \rho)g}{9\mu(\alpha)} \tag{3.12}$$

Where ρ and ρ_d are the densities of the continuous phase and droplet respectively, r_d is the droplet radius; and g is the acceleration due to gravity. The viscosity of the emulsion, μ (α), is a function of the oil cut, α

As mentioned in Chapter 2.1, v_y is the droplet velocity relative to the continuous phase. However, if the vertical movement of the continuous phase is neglected, then it can be used as an approximation to the absolute velocity. This assumption also entails neglecting all turbulence in the vertical direction.

3.8.3 Size Distribution/Droplet Size

In this Thesis, a normal distribution using the Rossin-Rammler [ANSYS Inc. Fluent User Guide and Fluent Theory Guide, version 14.0., 2011], function was assumed.

$$Y_d = e^{-(d/\bar{d})^n} \tag{3.13}$$

Where, Y_d is the volume or mass fractions of the droplets with diameter greater than d
This method requires tow parameters of the mean diameter and the spread parameter n. It is difficult to find the information on the size distribution for the mixtures of gas/oil/water, at this particular stage of separation. Nonetheless, Arnold and Stewart [22], suggested that, in the absence of field or laboratory data, water droplets larger than 500 μm in diameter should be separated resulting in 10% or less of water lost in the oil phase. In terms of the design of gas-oil separation, the recommended oil droplet diameter by Literature [22] within the band of 100-140 μm.

3.8.4 Viscosity and Concentration

The gravity separator is divided into three different phases having uniform concentration profiles. The emulsion phase is supposed to have an oil volume fraction equivalent to that of the incoming fluid, $\alpha = \alpha_{in}$. The separation process causes a pure oil phase to be formed in the top and a pure water phase at the bottom of the tank. As the liquid moves downstream in the gravity separator, the emulsion phase decreases while the two pure phases grow. This assumption is shown in Figure 3.4.

The concentration profile of the model is based on the assumption that all the droplets are moving with the same vertical velocity. The accuracy of this assumption reduces with increasing standard deviation in the droplet size distribution, because the buoyancy force is proportional to the droplet volume. This signifies that there is no oil droplets accumulation underneath the oil-emulsion bulk interface. Meaning that the coalescence process is relatively faster than the sedimentation process for the oil droplets and the continuous oil phase (shown in Chapter 2.3). Note that this based on the assumption that the sedimentation rate is relatively low ($g \approx 9.8\,\mathrm{m\,s^{-2}} \ll a_c$), with the droplets having to penetrate a relatively large bulk interface. The viscosity of the emulsion is considered to be dependent on the properties of the two liquids as well as the oil volume fraction.

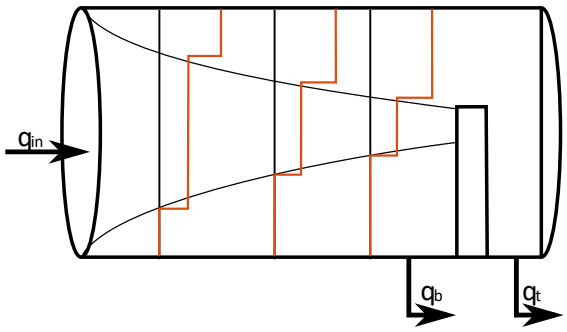

Figure 3.4: The concentration profile in the gravity separator model [33]. The red line signifies the oil volume fraction, α. The liquid is divided into three phases of:

1. The oil phase at the top with $\alpha = 1$
2. The emulsion phase in the middle with $\alpha = \alpha_{in}$.
3. The water phase on the bottom with $\alpha = 0$.

3.8.5 Oil Cut in the Product Streams

The estimation of the oil volume fractions of the product streams are done by finding the vertical distance, Δh, that a droplet inflowing the separator at the bottom travels during its residence time in the separator. A droplet at the lower part of the separator (below H_w) travels the vertical distance of;

$$\nabla h = \frac{v_x}{v_y} L \quad 3.4 \qquad (3.14)$$

where v_x and v_y are the horizontal and vertical velocities of the droplet respectively, L is the horizontal distance between the inlet and the weir.

The situation shown in Figure 3.5 will arise if all the droplets travel with the same vertical velocity. Figure 3.5a illustrates the cross section of the separator at the inlet, where the whole liquid is assumed as an oil-in-water emulsion. In Figure 3.5b, typifies the end of the separator for all droplets moving with the same vertical distance, Δh. In practice, the droplets colliding with the ceiling accumulate and form a continuous stream of oil phase at the top as in Figure 3.5c. It is important to note that the liquid above H_w might have a different horizontal velocity from the liquid below H_w, since the illustration is not an exact representation. The droplets crossing the horizontal plane at the height H_w have different residence times and consequently transit different vertical distances. Nevertheless, the relevant information required to estimate the outlet composition is the aggregate of oil droplets that cross the horizontal plane.

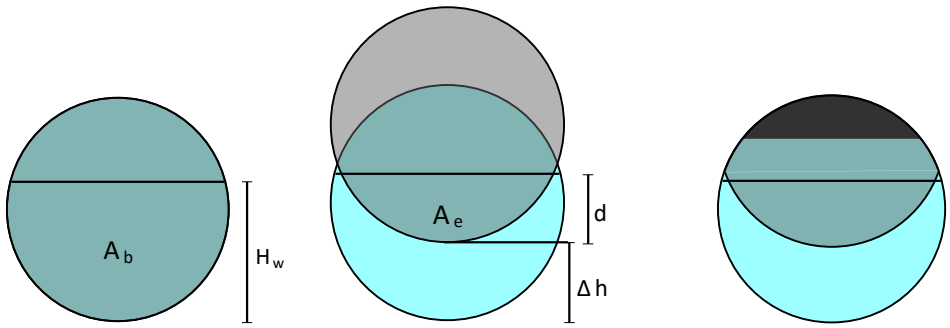

(a) At beginning of separator. (b) At the end separator Hypothetical case. (c) At the end of separator. " Actual case".

Figure 3.5: Cross section of the gravity separator at the beginning and end of the vessel. The emulsion (grey) travels vertically at a distance Δh during its residence time in the device. The pure oil phase (black) forms at the top while the pure water phase (light blue) forms at the bottom of the vessel [33].

The volume of the of oil residue remaining at the bottom-end of the separator is defined by the limited circular segment of $d = H_w - \Delta h$, see Figure 3.11b. The area of the circular segment is given as:

$$A_e = \frac{R^2}{2}\left[2\cos^{-1}\left(\frac{R-d}{R}\right) - \sin\left(2\cos^{-1}\left(\frac{R-d}{R}\right)\right)\right] \qquad (3.15)$$

The oil volume fraction for the bottom outlet, α_b, is therefore given as:

$$\alpha_b = \alpha_{in}\frac{A_e}{A_b} \qquad (3.16)$$

where α_{in} is the oil volume fraction of the stream at the inlet and A_b is the cross section area of the lower part of the gravity separator given by equation 3.15. The oil volume fraction of the top outlet is gotten from component-mass balance as:

$$\alpha_t = \frac{1}{q_t}\left[\alpha_{in}\ q_{in} - \alpha_b\ q_b\right] \qquad (3.17)$$

Where q_{in}, q_b and q_t are the volumetric flow rates of the inlet, bottom and top outlets respectively.

3.9 Model Input

A number of input/design parameters were adopted from different published works on Horizontal three-phase separators.

3.9.1 Fluid Properties

The input data from Table 3.2 was gotten from a similar design [23]. The composition of the oil and water in Table 3.1 was chosen as a close approximate to what is obtainable from the industry, the work of Gjengedal [13], was used.

Component	Oil Composition [Mol]	Water Composition [Mol %]
H20	0.004	0.999
N2	0.016	0.000
CO2	0.022	0.001
C1	0.604	0.000
C2	0.076	0.000
C3	0.048	0.000
i-C4	0.021	0.000
n-C4	0.021	0.000
i-C5	0.015	0.000
n-C5	0.015	0.000
C6	0.020	0.000
C7	0.024	0.000
C8	0.023	0.000
C9	0.016	0.000
C10	0.014	0.000
C11	0.010	0.000
C12+	0.051	0.000

Table 3.1: Typical Reservoir composition of Oil & Water [13]

Streams	Well Oil	Well Water
Temp. (°C)	76.85	76.85
Press. (Bar)	100	100
Density (kg/m^3)	813.464	1015.097

Table 3.2: Input Parameters for the HYSYS Three Phase Horizontal Separator

3.9.2 Gravity Separator Dimension

The geometry and physical dimension in Figure 3.6 was used for the modelling.

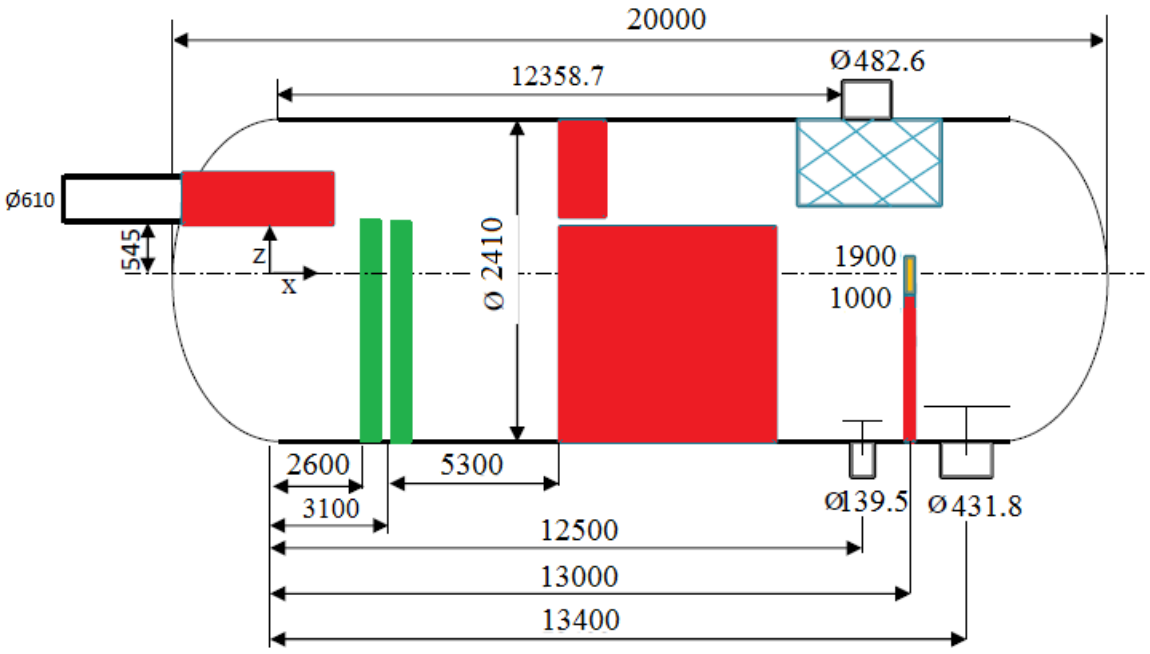

Figure 3.6: Physical dimensions and Geometry of the horizontal gravity separator [11]

4.0 Results and Discussion of Results

The objective of this thesis was to model a three-phase horizontal subsea separator in HYSYS. The gravity separator (discussed in section 3) was modelled with parameters from Literatures [11, 23]. It is therefore necessary to state that the model predictions are reasonable qualitative responses to changes in the input variables. Nonetheless, the predictions are not expected to be accurate quantitative values of the product streams purities. Several simulations were performed, on the HYSYS separator model, by varying the flow rates, oil cuts and residence time (factor) of the inlet stream: then, the separator efficiency was investigated by observing the purities of the product streams. The results obtained were presented and discussed in the following sections.

4.1 Effect of Flow Rate on Products Purity

Simulations were performed by varying the flow rates of the inlet stream for oil cuts of 0.4 and 0.5. Results of the simulations are discussed in the subsections for the various products.

4.1.1 Effect of Flow Rate on Gas Product Purity

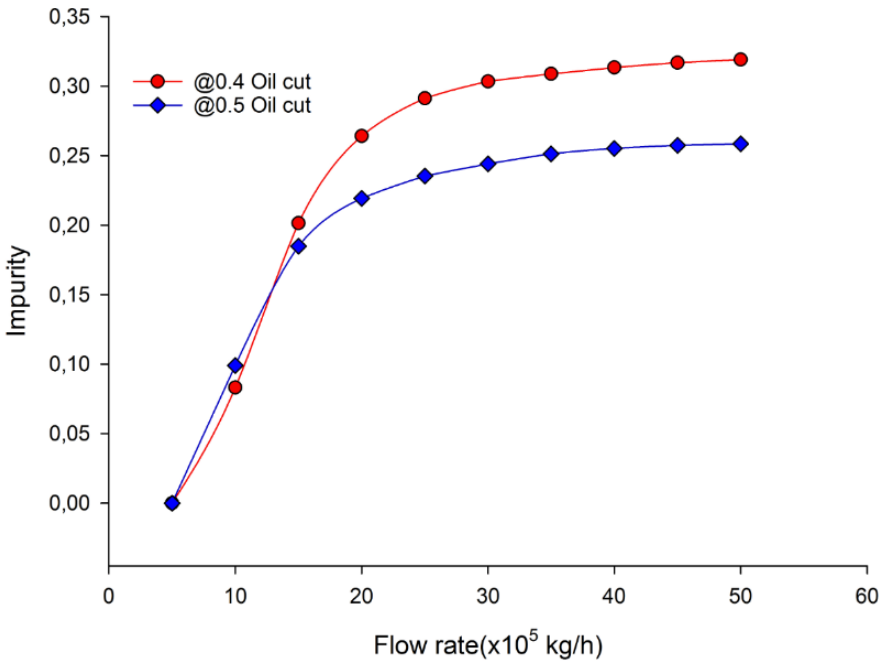

Figure 4.1: Impurity of Gas Product Vs the Flow Rate of the Mixed Stream at Oil cuts of 0.4 & 0.5

Figure 4.1 clearly shows that the impurity of the Gas outlet increases with increasing flow rates. That means the separator efficiency decreases with increasing flow rate. It also illustrates that the flow with the lower oil cut of 0.4 gives a better separation efficiency than the other with same flow rate at 0.5 Oil cut. Other simulations performed confirmed similar trends.

4.1.2 Effect of Flow Rate on Oil Product Purity

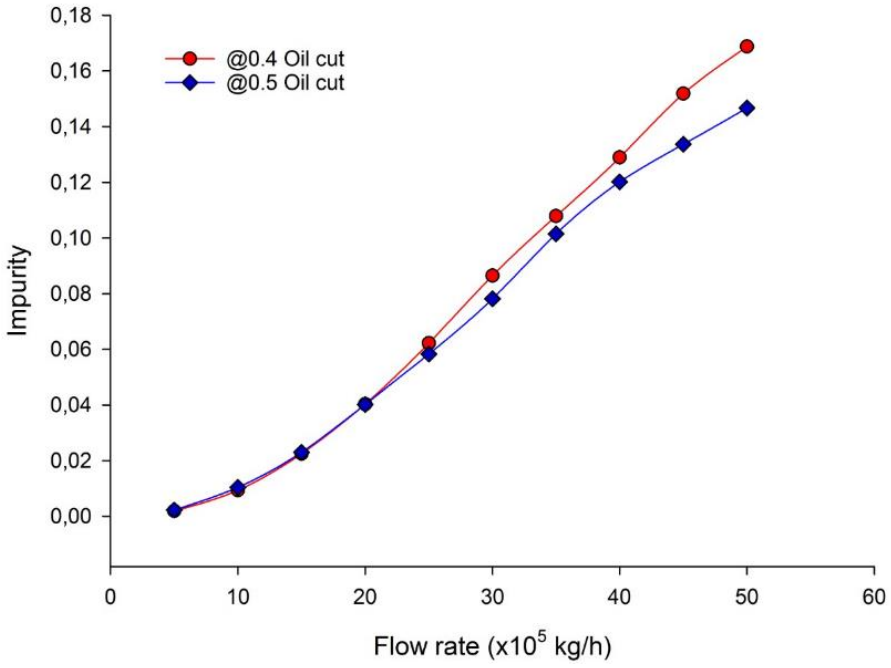

Figure 4.2: Impurity of the Oil Product Vs the Flow Rate of the Mixed Stream at Oil cuts of 0.4 & 0.5.

As shown in figure 4.2, the impurity of the Oil stream increases with flow rates. That means the separator efficiency decreases with flow rate. The impurities of the Oil streams at oil cut of 0.4 and 0.5 are nearly the same until above $20x10^5$ kg/h. Overall, the flow rate with the lower oil cut of 0.5 gives lower impurities compared to the same flow rate at 0.4 Oil cut.

4.1.3 Effect of Flow Rate on Water Product Purity

For figure 4.3, the impurity of the water stream increases with flow rates. That means the separator efficiency decreases with flow rate. The impurities of the water streams at oil cut of 0.4 and 0.5 are nearly the same until above $20x10^5$ kg/h. Overall, the flow rate with the lower oil cut of 0.5 gives lower impurities compared to the same flow rate at 0.4 Oil cut.

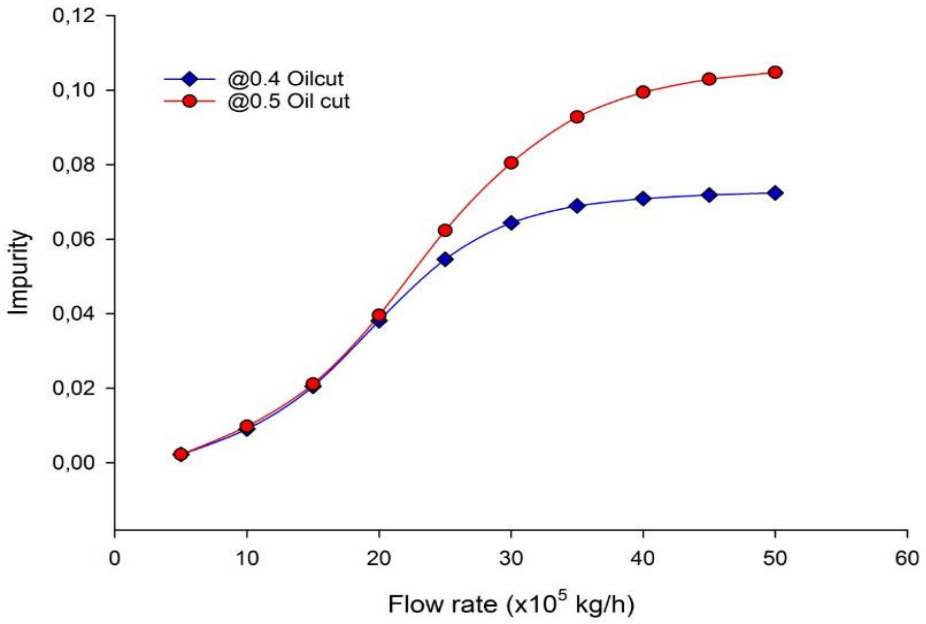

Figure 4.3: Impurity of the Water Product Vs the Flow Rate of the Mixed Stream at Oil cuts of 0.4 & 0.5

4.2 Effect of Residence Time on Purity of Product Streams

Simulation were perfomed by changing the residence time of the different phases. The results obtained are given and explain in the subsections.

4.2.1 Effect of Residence Time on Oil Product Purity

Figure 4.4 shows that the impurity of Oil product decreases with increasing residence time of the Oil phase, meaning that the separation efficiency of the separator increases with increasing residence time. This allows plenty time for coalescence of droplets and dispersions from other

phases of gas and water and also to further settle out from gravitational buoyancy. This processes contribute greatly to improving the separation and separator efficiency as discussed in sections 2.6, 2.7 and 2.8. Similar pattern was observed from additional simulations.

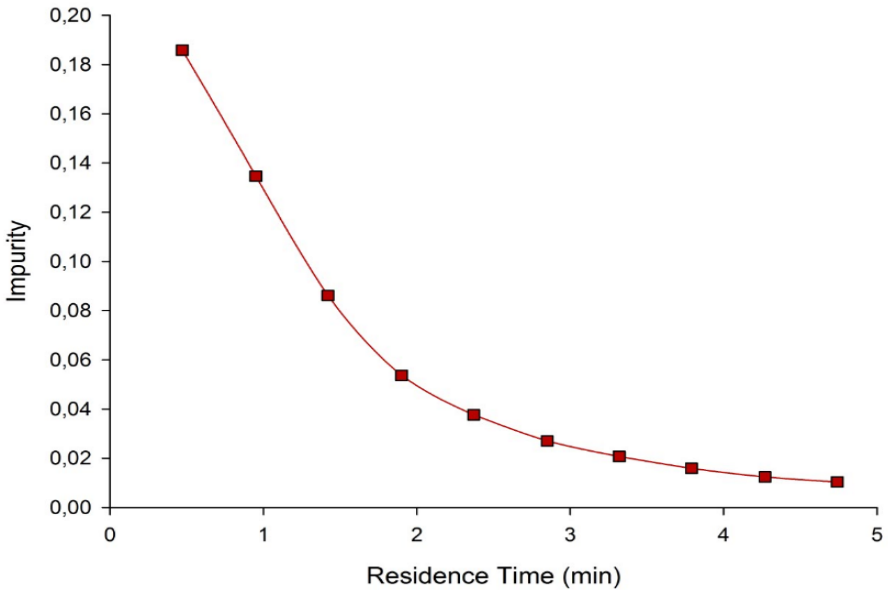

Figure 4.4: Impurity of the Oil Product Vs Residence Time of the Oil in the Gravity Separator

4.2.2 Effect of Residence Time on Water Product Purity

Similarly, figure 4.5 shows a familiar behavior as in figure 4.4. i.e., the impurity decreases with increasing residence time of the water phase, meaning that the separation efficiency of the separator increases also with increasing residence time.

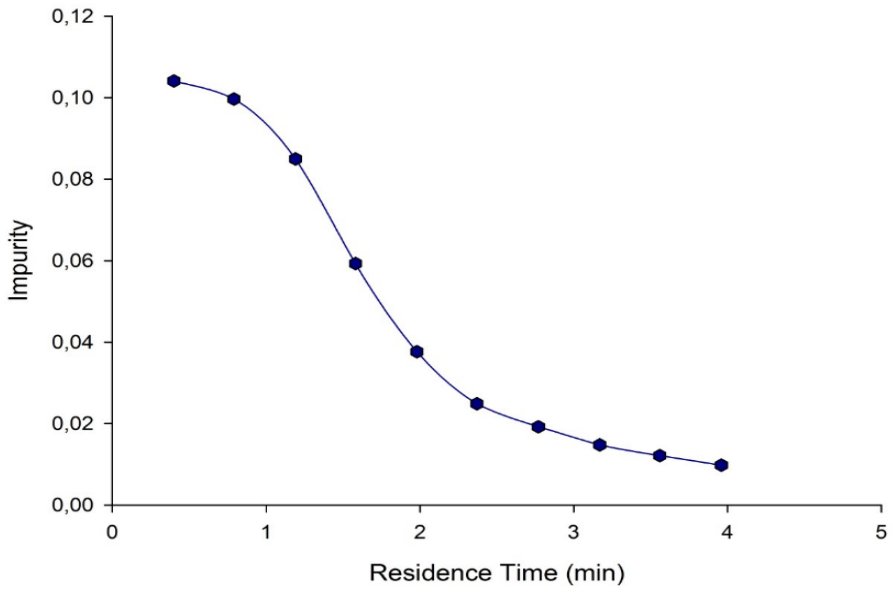

Figure 4.5: Impurity of Water Product Vs Residence Time of the Water in the Gravity Separator

4.2.3 Effect of Residence Time on Gas Product Purity

Figure 4.6 shows unexpected result. This might be as a result of the relatively small volume of the gas for each varying flow rates.

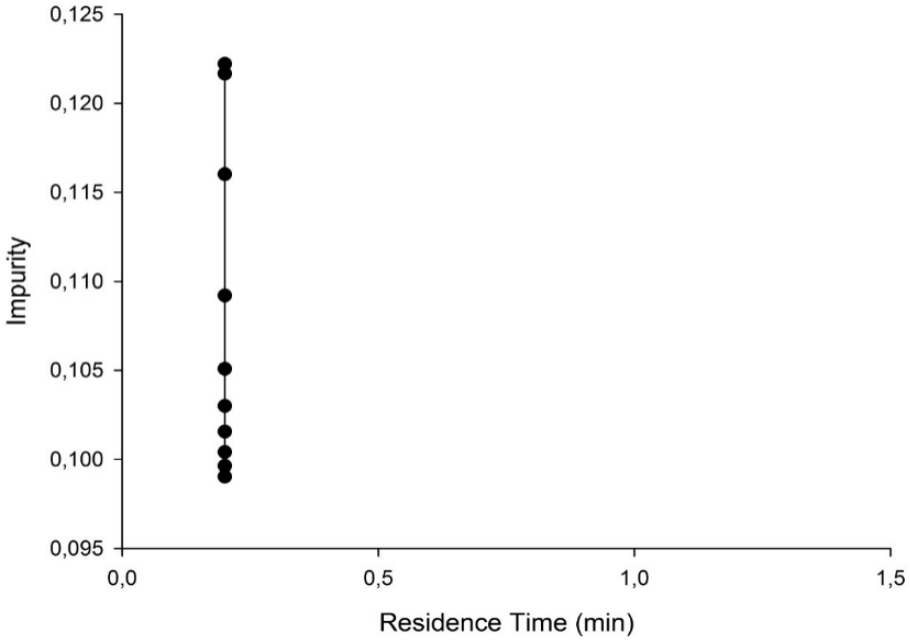

Figure 4.6: Impurity of the Gas Product Vs Residence Time of the Gas in the Gravity Separator

4.3 Effect of Oil cut on Purity of Product Streams

Simulation were perfomed by changing the oil cuts of the mixed stream. The results obtained are given and explain in the subsections.

4.3.1 Effect of Oil cut on Gas Product Purity

In figure 4.7, it is shown that the impurities of the Gas streams at both flow rates of (20 & 25) x10^5 kg/h increased initially with increasing oil cut. This trend continued until at an oil cut of 0.3 where a decrease starts for the remaining oil cuts simulations.

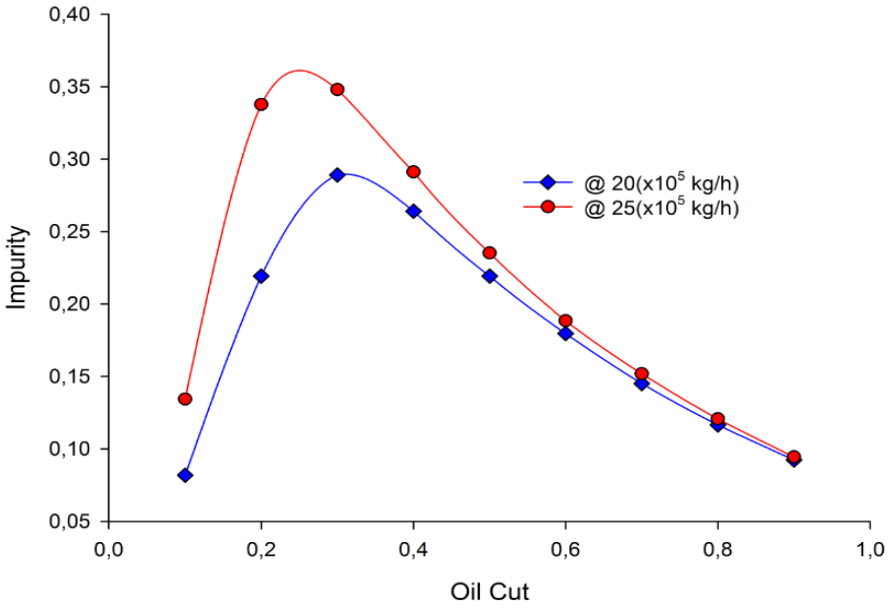

Figure 4.7: Impurity of Gas Product Vs Oil cut at Flow rates of (20 & 25) x105 kg/h

4.3.2 Effect of Oil cut on the Purity of Oil Product

Figure 4.8 shows an initial decrease in the impurities of both Oil outlets at flow rates of (20 & 25) x10^5 kg/h, which symbolizes increased separator efficiency) This trend was sustained until at an oil cut of 0.5 where it began to increase with increasing oil cuts. The initial descent was because of the increase in the oil fractions as against a decrease in the water fractions in the mixed stream.

However, It is most likely that, the sudden increase of the impurities for both streams could be because of phase inversion (50%). Where the Oil-in-Water emulsion suddenly changes into water-in-Oil emulsions as a result of increase in the oil fractions as against a decrease in the water fractions. The higher impurities in the higher flow of 25 $x10^5$ kg/h over 20 $x10^5$ kg/h is expected because of the relative larger volume fractions in the emulsion. Another probable explanation may be that the viscosity which is highest at the phase inversion in turn decreases the separator efficiency.

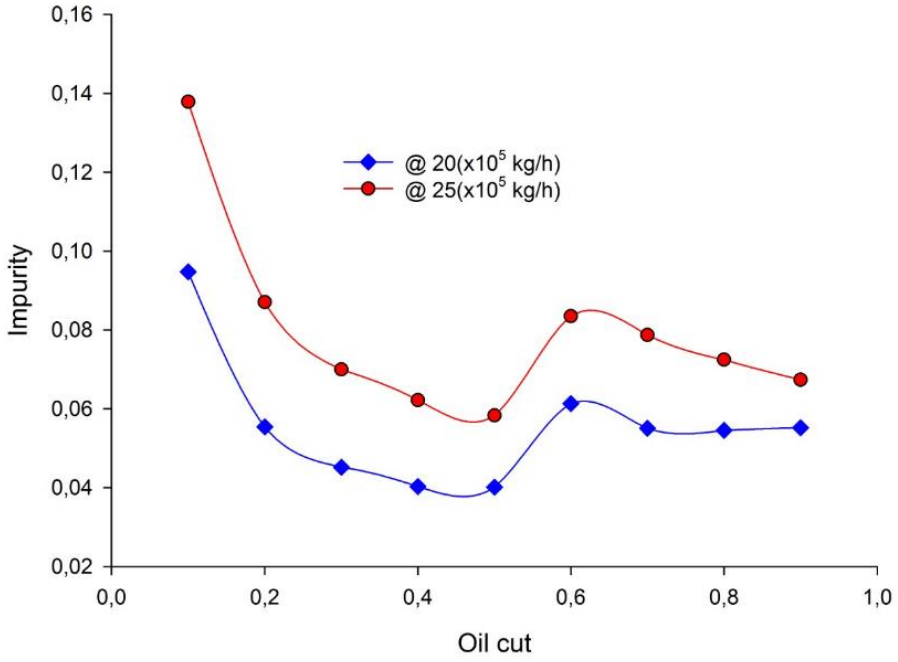

Figure 4.8: Impurity of Oil Product Vs Oil cut at Flow rates of (20 & 25) x105 kg/h

4.3.3 Effect of Oil cut on the Purity of Water Product

Figure 4.9 illustrates how the impurities increases with increasing oil cut for both streams at flow rates of (20 & 25) $x10^5$ kg/h. And the impurities increased from 0.5 to 0.6 oil cut and began a decrease. Initial increase was as result of increasing fractions of oil for oil-in-water emulsion. The trend changed after 0.6 oil cut to a decrease because of phase inversion of oil-in-water emulsion

to water-in-oil emulsion. This is as a result of subsequent decrease in water fraction and increase in oil fractions.

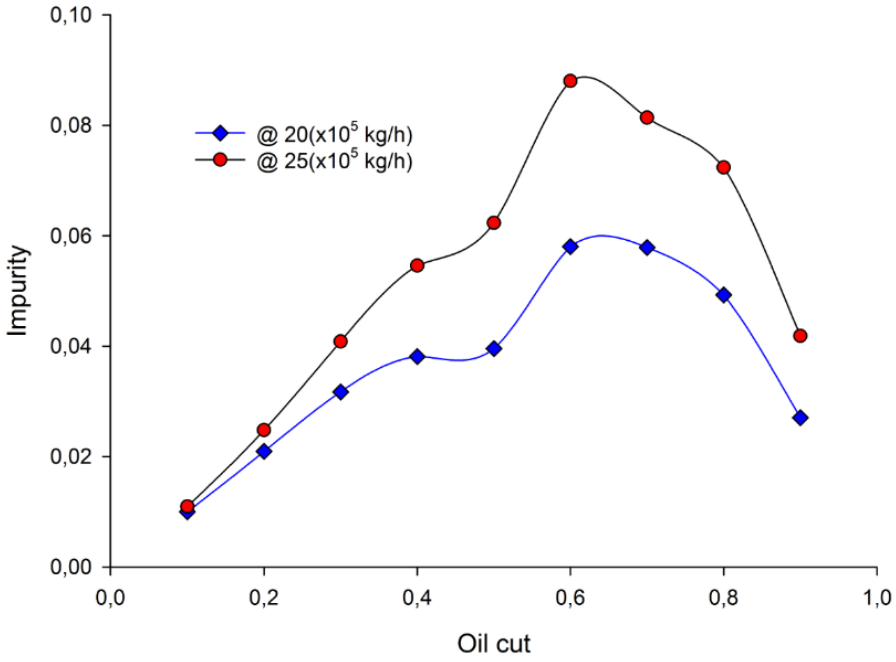

Figure 4.9: Impurity of Water Product Vs Oil cut at Flow rates of (20 & 25) x105 kg/h

5 Conclusion and Future Work

5.1 Conclusion

The objective of this thesis is to develop steady state and dynamic models of a three phase subsea separator in HYSYS. Then, comparatively investigate the separator model for optimization and control relative to a similar work by Tyvold.

Several simulations were performed by varying the flow rates, oil cuts and residence time (factor) of the inlet stream: then, the separator efficiency was investigated by observing the purities of the product streams. The residence time, which cannot be changed directly, was varied by changing the residence time factor of the HYSYS separator model from 0.9 to 0.1. This in turn changes the residence time of the phases accordingly. The purities of the product products stream did not meet the Regulatory specification of 30 ppm as discussed in section 2.3. This, probably, indicating a need for integration of additional (compact) separator(s). However, the model generally showed an acceptable response to the input parameters compared to the theories from literatures as discussed in section 2. Some of these results also agree with previous work of Tyvold. An experimental data would have been important in comparing and validating the results of the model. The Dynamic model converged but it gives negative flow rates at the inlet of the separator. This might be due to high pressures at the downstream and/or it requires a well-defined boundary conditions from the field or experiment. Hence, I could not conclude on the dynamic model because this will need experimental/field data which I was unable to access.

5.2 Further Work

The aim of future works should be to implement control for the models, and obtain data from experiment and/or the field to fit the models. In addition, the effect of droplets sizes on separator efficiency should be investigated. The Dynamic model should also be improved upon.

Bibliography

[1] Anres, S., Abrand S., Butin N., Evans W., Bigeonneau D., 2011. New Solutions for Subsea Produced Water Separation and Treatment in Deepwater. Offshore Technology Conference in Brasil.

[2] AspenTech. (2009), Aspen HYSYS Customized Guide. Version 2006.5, Aspen Technology, INC, Cambridge.Downloaded from: http://support.aspentech.com/Public/Documents/Engineering/Hyprotech/2006.5/AspenHYSY S2006_5-Cust.pdf [cited 18.12.2015]

[3] Arirachakaran, S., Oglesby, K., Malinowsky, M., Shoham, O., Brill, J., 1989. An analysis of oil/water flow phenomena in horizontal pipes. In: SPE Production Operations Symposium, 13-14 March, Oklahoma City, Oklahoma. Society of Petroleum Engineers, SPE. https://www.onepetro.org/conference-paper/SPE-18836-MS.

[4] Balakrishna, S., Biegler, L. T., 1992. Targeting strategies for the synthesis and energy integration of nonisothermal reactor networks. Industrial & Engineering Chemistry Research 31 (9), 2152–2164. http://dx.doi.org/10.1021/ie00009a013.

[5] Barnea E; Mizrahi J. A Generalized Approach to the Fluid Dynamics of Particulate Systems. *The Chemical Engineering Journal, 5 (1973)* 171-189 171. Elsevier Sequoia S.A., Lausanne. Printed in the Netherlands**.**

[6] Bringedal, B., Ingebretsen T., Haugen T., 1999. Subsea Separation and Reinjection of Produced Water. Offshore Technology Conference held in Houston. Texas, U.S.A.

[7] Constantinides, A., Mostoufi, N., 1999. Numerical Methods for Chemical Engineers with MATLAB Applications. Prentice Hall PTR, Prentice-HAll Inc., Upper Saddle River, New Jersey.

[8] Davies, J., 1985. Drop sizes of emulsions related to turbulent energy dissipation rates. Chemical Engineering Science 40 (5), 839 – 842. http://www.sciencedirect. com/science/article/pii/ 0009250985850363. May, 2016

[9] Devegowda, D., Scott S. L. An Assessment of Subsea Production Systems. SPE Annual Technical Conference and Exhibition held in Denver. Colorado, U.S.A. 1999

[10] Dirkzwager, M., December 1996. A New Axial Cyclone Design for Fluid-Fluid Separation. Ph.D. thesis, Delft University of Technology.

[11] Evert O; Kyaerner S; Matthew J. Optimal Design of Two- and Three-Phase Separators: A Mathematical Programming Formulation Optimal Design. SPE Annual Technical Conference and Exhibition held in Houston, Texas, October 1999.

[12] FMC Technologies (2015), Subsea separation [online] Available from: http://www.maximizerecovery.com/Technologies/subsea-separation. April 2016

[13] Gjengedal C., 2013. Subsea Separation of Water and Oil. MSc. Specialization Project Norwegian University of Science and Technology.

[14] Gruehagen, Henning, Lim D, 2009. Subsea Separation and Boosting - An Overview of Ongoing Projects. » SPE Asia Pacific Oil and Gas Conference and Exhibition held in Jakarta. Indonesia: Society of Petroleum Engineers.

[15] GPSA Engineering data Book, 2004. 12th ed., vol.1, Section 7. Gas Processor Suppliers Association(GPSA). Tulsa, OK, USA.

[16] GPSA Eng. Data**:** Perry, Robert H., Editor, Chemical Engineers' Handbook, 5th Edition, McGraw-Hill Book Company, 1973, Chapter 5, p. 5–61-65.

[17] GPSA: American Petroleum Institute, RP 521, Guide for Pressure Relieving and Depressuring Systems, 4th Edition, March 1997, p. 64

[18] Hamid, M.K.A. (2007), HYSYS: An Introduction to Chemical Engineering Simulation.

[19] Hinze, J. O., 1955. Fundamentals of the hydrodynamic mechanism of splitting in dispersion processes. AIChE Journal 1 (3), 289–295.

[20] Ishii, M., Zuber, N., 1979. Drag coefficient and relative velocity in bubbly, droplet or particulate flows. AIChE Journal 25 (5), 843–855

[21] Jahnsen, O. F., Storvik M., 2011. Subsea Processing & Boosting in a Global Perspective. Offshore Mediterranean Conferende and Exhibition in Ravenns. Italy.

[22] K. Arnold and M. Stewart, Surface Production Operations, Volume 1: third Edition, Design of Oil-Handling Systems and Facilities, USA: Gulf Professional Publishing, 2008

[23] Kharoua N; Khezzar L; Sadaawi H. CFD Modelling of a Horizontal Three-Phase Separator: A Population Balance Approach**,** American Journal of Fluid Dynamics 2013, 3(4): 101-118

[24] Maria J; Wang L; Wassenhove W. Aspen HYSYS Property Packages Overview and Best Practices for Optimum Simulations Aspen Process Engineering Webinar October 17, 2006

[25] Lucas R; Dharmendra T. Real Separator Guide, Version 1.0. July 2004

[26] MathWorks, Inc., 2015. Documentation: fmincon. Accessed:201505-29. http://se.mathworks.com/help/optim/ug/fmincon.html.

[27] McClimans, O., Fantoft, R., 2006. Status and new developments in subsea processing. In: Offshore Technology Conference, 1-4 May, Houston, Texas, USA. (https://www.onepetro.org/conference-paper/OTC-17984-MS).

[28] Moreno-Trejo, J., Markeset, T., 2012. Identifying challenges in the development of subsea petroleum production systems. In: Frick, J., Laugen, B. (Eds.), Advances in Production Management Systems. Value Networks: Innovation, Technologies, and Management. Vol. 384 of IFIP Advances in Information and Communication Technology. Springer Berlin Heidelberg, pp. 287–295. (http://dx.doi.org/10.1007/978-3-642-33980-6_33)

[29] Mørk, P. C., 1999. Overflate og kolloidkjemi: grunnleggende prinsipper og teorier. Norwegian University of Science and Technology, Department of Chemical Engineering, Trondheim, Norway.

[30] Najafi, A., Mousavian, S., Amini, K., 2011. Numerical investigations on swirl intensity decay rate for turbulent swirling flow in a fixed pipe. International Journal of Mechanical Sciences 53 (10), 801 – 811. (http://www.sciencedirect.com/science/article/pii/)

[31] Nel Technology for Life. Subsea Separation Systems [online]. Available from: http://www.tuvnel.com/_x90lbm/Subsea_separation_systems.pdf. April 2016

[32] Petroleum Safety Authority Norway, 2001. Regulations relating to conducting petroleum activities. Accessed: December 2015. http://www.ptil.no/aktivitetsforskriften/ aktivitetsforskriften-e2007-n-article3868-379.html.

[33] Preben, F. Tyvold., 2015. Modeling and Optimization of a Subsea Oil-Water Separation

[34] Rassenfoss, Stephen 2011, Growing Offshore Water Production Pushes Search for Subsea Solutions. Aker Solutions.

[35] Rasmussen, A. W., 2003. Enhanced Oil Recovery by Retrofitting Subsea Processing. Offshore Europe 2003 held in Aberdeen.

[36] Sherman, P., 1962. The viscosity of emulsions. Rheologica Acta 2 (1), 74–82. http://dx.doi.org/10.1007/BF01972558.

[37] Simon D; William B; Rune M; Roger O. Experience to Data and Future Opportunities for Subsea Processing in Statoil. Offshore Technology Conference, Texas, 2010

[38] Skogestad, S., 2000. Plant wide control: the search for the self-optimizing control structure. Journal of Process Control 10 (5), 487 – 507. http://www.sciencedirect.com/

[39] Slot, J. J., October 2013. Development of a Centrifugal In-Line Separator for Oil-Water Flows. Ph.D. thesis, University of Twente.

[40] Statoil ASA, 2015. Subsea processing on Tordis. Accessed: 2015-0603.

Available from:http://www.statoil.com/en/TechnologyInnovation/FieldDevelopment/Ab

outSubsea/SubseaProcessingOnTordisIOR/Pages/default.aspx.

[41] Underwater Technology Foundation (2015), Subsea History [online]

Available from: http://www.utc.no/utf/om_subsea/subsea_history/

[42] Van Campen, L., January 2014. Bulk Dynamics of Droplets in Liquid Liquid Axial Cyclones. Ph.D. thesis, Delft University of Technology.

[43] Van Campen, L., Mudde, P. R., dr.ir. J.J. Slot, prof.dr.ir. H.W.M. Hoeijmakers, 2012. A numerical and experimental survey of a liquid-liquid axial cyclone. International journal of chemical reactor engineering 10 (1). http://doc.utwente.nl/83139/

[44] Vu, V. K., Fantoft R., Chris S., Gruehagen H., 2009. Comparison of Subsea Separation Systems. Offshore Technology Conference, Houston, USA

[45] Woelflin, W., 1942. The viscosity of crude-oil emulsions. In: Drilling and Production Practice, 1 January, New York, New York. American Petroleum Institute, API. https://www.onepetro.org/conference-paper/API-42-148

[46] Yang, M., 2012. Challenges for Water Quality Measurement for Produced Water Handling Subsea. Offshore Technology Conference held in Houston. Texas, U.S.A.

[47] http://www.chemwork.org/PDF/board/how%20to%20define%20liquid-%20liquid%20separation.pdf. June, 2016

[48] https://lhd52.files.wordpress.com/2011/09/group-6-separation-operations.pdf. July 2016

Appendix A: Qualitative Simulation Results

S/N	Flow rate of mixed stream (10^5 kg/h) @0.4 Oilcut	Impurity of Product Streams		
		Gas	Oil	Water
1	5	0.0000000	0.0019187	0.0022213
2	10	0.0831468	0.0093322	0.0090658
3	15	0.2014376	0.0224689	0.0205117
4	20	0.2641222	0.0402862	0.0381243
5	25	0.2912235	0.0621780	0.0546071
6	30	0.3033494	0.0864877	0.0643999
7	35	0.3088309	0.1079066	0.0689487
8	40	0.3133371	0.1289649	0.0708935
9	45	0.3168159	0.1518504	0.0718858
10	50	0.3190894	0.1687793	0.0724158

Table A.1: Impurities of Product Streams versus Flow rates of Mixed Stream @ 0.4 Oilcut

SN	Flow rate of mixed stream (10^5 kg/h) @0.5 Oilcut	Impurity of the product Streams		
		Gas	Oil	Water
1	5	0.0000000	0.0022846	0.0022423
2	10	0.0990248	0.0104067	0.0097900
3	15	0.1849651	0.0229647	0.0211320
4	20	0.2193186	0.0401512	0.0395579
5	25	0.2353007	0.0582931	0.0623387
6	30	0.2441334	0.0782075	0.0804808
7	35	0.2513186	0.1015149	0.0927821
8	40	0.2552202	0.1201874	0.0994090
9	45	0.2574232	0.1337132	0.1029040
10	50	0.2584884	0.1467330	0.1047503

Table A.2: Impurities of Product Streams versus Flow rates of Mixed Stream @ 0.5 Oilcut

SN	Oilcut of mixed stream @ Inlet Flow rate of 20 (10^5 kg/h)	Impurity of the product Streams		
		Gas	Oil	Water
1	0.1	0.0818767	0.0947596	0.0100039
2	0.2	0.2192872	0.0554315	0.0209431
3	0.3	0.2891372	0.0452073	0.0317153
4	0.4	0.2641222	0.0402862	0.0381243
5	0.5	0.2193186	0.0401512	0.0395579
6	0.6	0.1796439	0.0613101	0.0580416
7	0.7	0.1451785	0.0550536	0.0578887
8	0.8	0.1166279	0.0545501	0.0492935
9	0.9	0.0923914	0.0551939	0.0270627

Table A.3: Impurities of Product Streams versus Oilcuts of Mixed Stream @ Inlet Flow rate 20 (10^5 kg/h)

SN	Oilcut of mixed stream @ Inlet Flow rate of 25 (10^5 kg/h)	Impurity of the product Streams		
		Gas	Oil	Water
1	0.1	0.1343960	0.1378335	0.0109618
2	0.2	0.3376937	0.0870881	0.0247866
3	0.3	0.3479885	0.0699479	0.0408215
4	0.4	0.2912235	0.0621780	0.0546071
5	0.5	0.2353007	0.0582931	0.0623387
6	0.6	0.1884177	0.0835213	0.0880167
7	0.7	0.1518704	0.0786938	0.0813753
8	0.8	0.1207343	0.0724422	0.0723902
9	0.9	0.0945017	0.0673544	0.0418303

Table A.4: Impurities of Product Streams versus Oilcuts of Mixed Stream @ Inlet Flow rate 25 (10^5 kg/h)

SN	Residence Time of Gas Phase (min)	Impurity of Gas Product
1	0.2	0.099025
2	0.2	0.099637
3	0.2	0.100404
4	0.2	0.101557
5	0.2	0.102994
6	0.2	0.105083
7	0.2	0.109208
8	0.2	0.116013
9	0.2	0.121660
10	0.2	0.122206

Table A.5: Impurities of Gas Product versus Residence Time of Gas Phase

SN	Residence Time of Oil Phase (min)	Impurity of Oil Product
1	4.74	0.010407
2	4.27	0.012465
3	3.79	0.015938
4	3.32	0.020730
5	2.85	0.027044
6	2.37	0.037689
7	1.9	0.053730
8	1.42	0.086165
9	0.95	0.134652
10	0.47	0.185882

Table A.6: Impurities of Oil Product versus Residence Time of Oil Phase

SN	Residence Time of Water Phase(min)	Impurity of Water Product
1	3.96	0.009790
2	3.56	0.012139
3	3.17	0.014770
4	2.77	0.019223
5	2.37	0.024871
6	1.98	0.037640
7	1.58	0.059310
8	1.19	0.084995
9	0.79	0.099707
10	0.4	0.104122

Table A.7: Impurities of Water Product versus Residence Time of water Phase

Appendix B: HYSYS Model Files

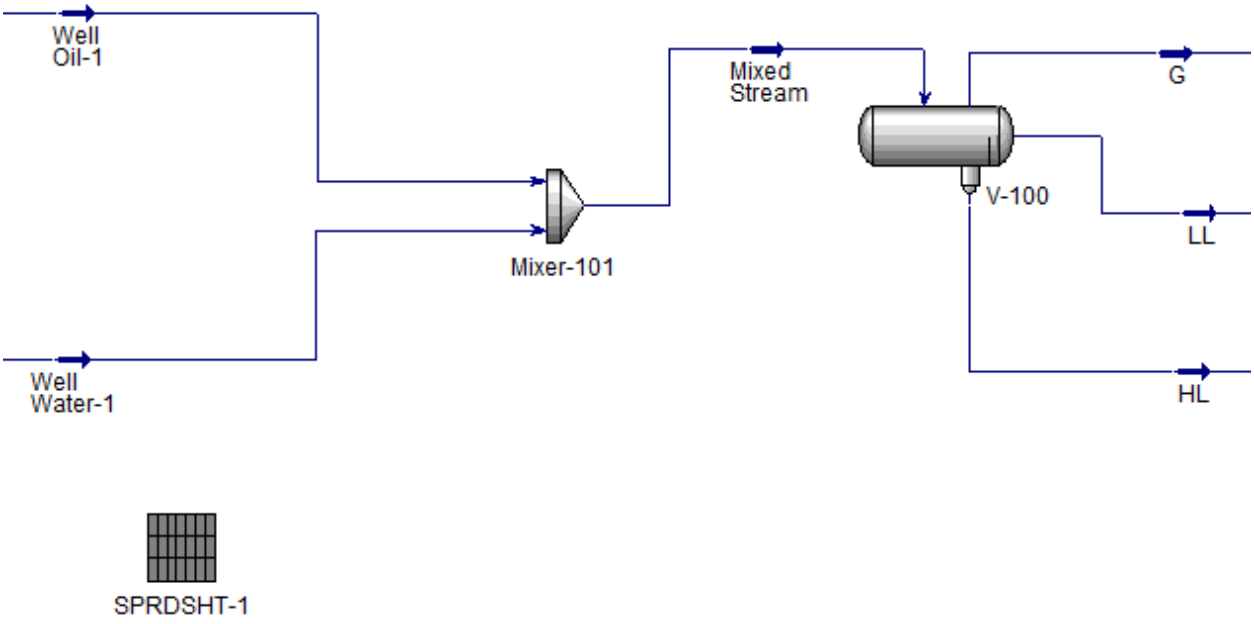

Figure B.1: Flowsheet of the Steady-State Model of the Horizontal Three-Phase Subsea Separator

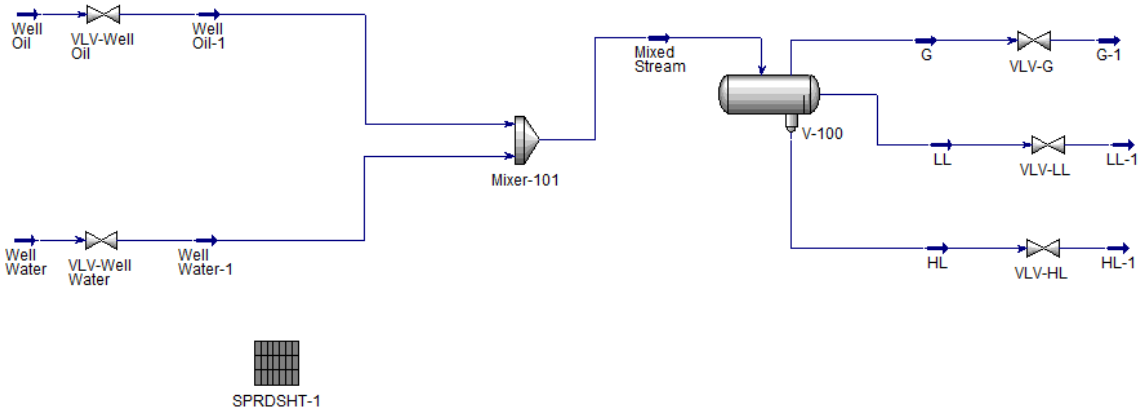

Figure B.2: Flowsheet of the Dynamic-State Model of the Horizontal Three-Phase Subsea Separator

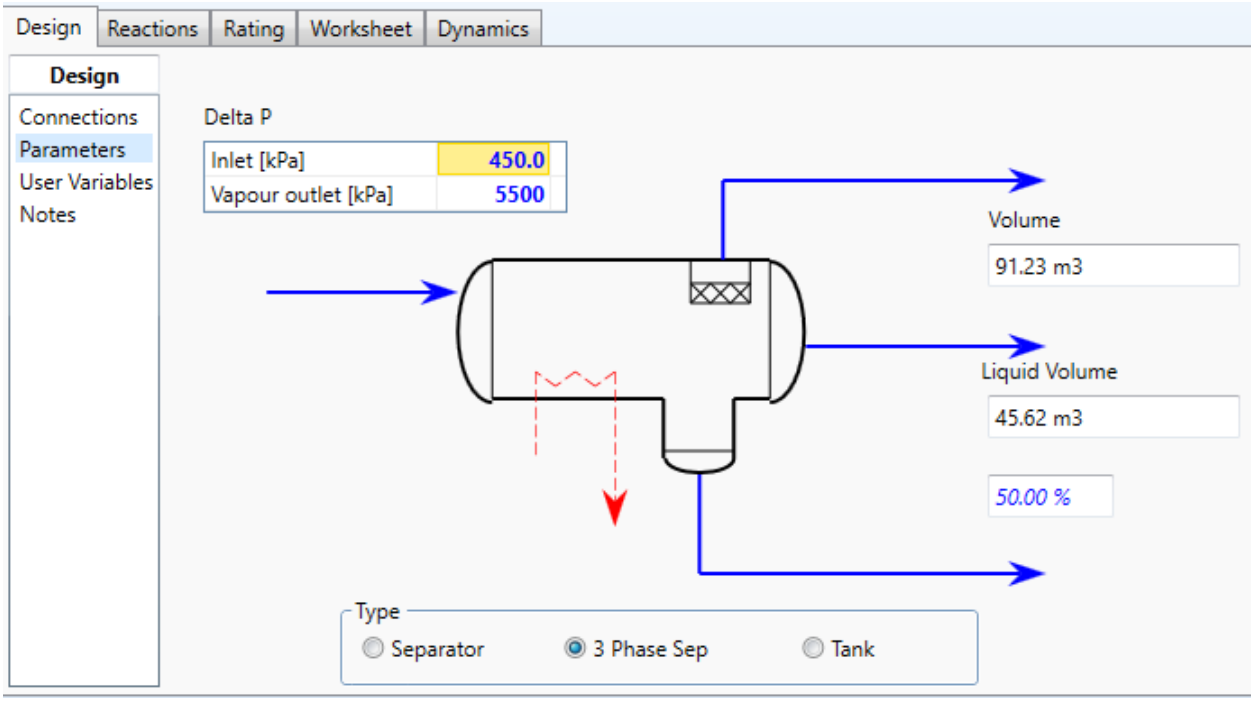

Figure B.3: Design Parameter of the Horizontal Three-Phase Subsea Separators (Dyanamic & Steady-State Models)

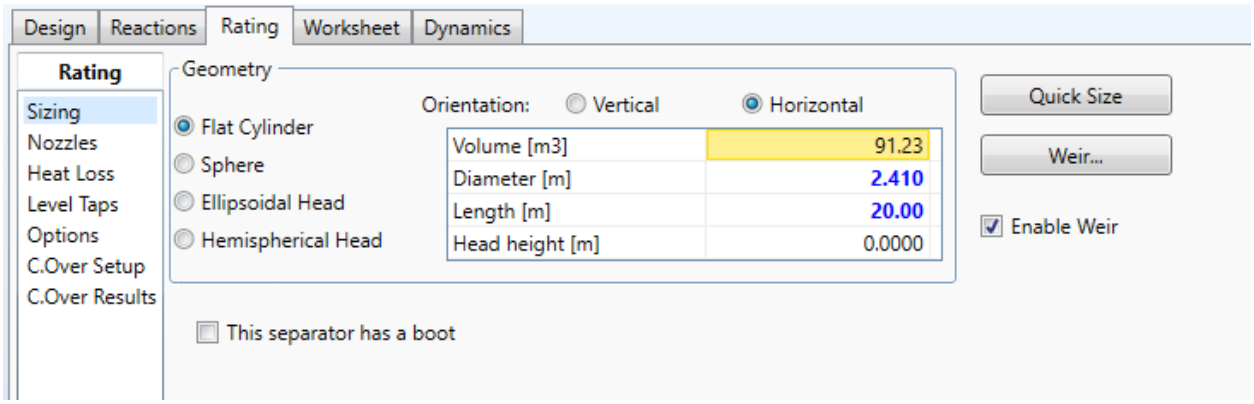

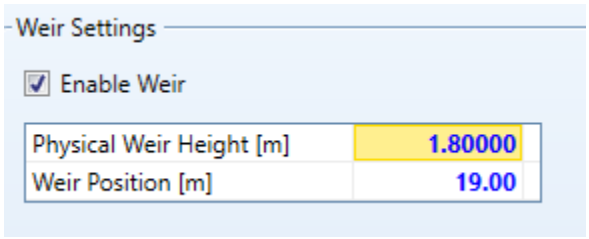

Figure B.4: Basic Dimensions of the Horizontal Three-Phase Subsea Separators

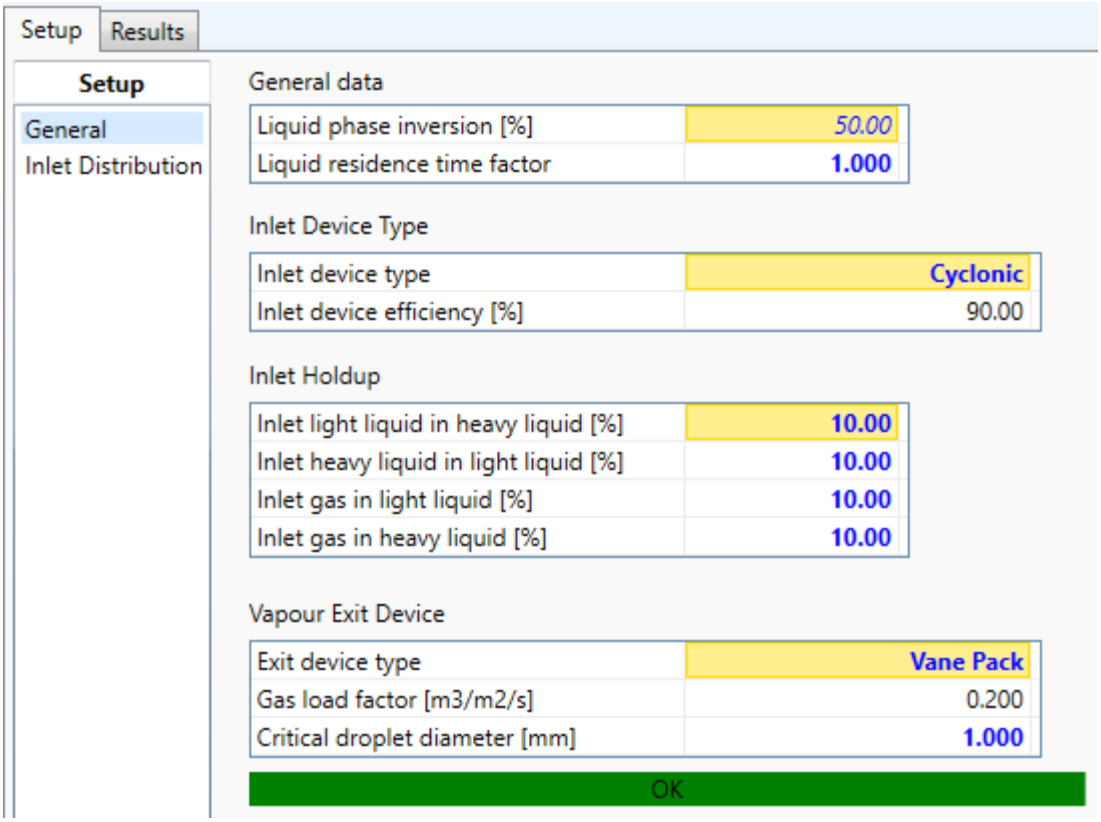

Figure B.5: General specifications of the separators internals

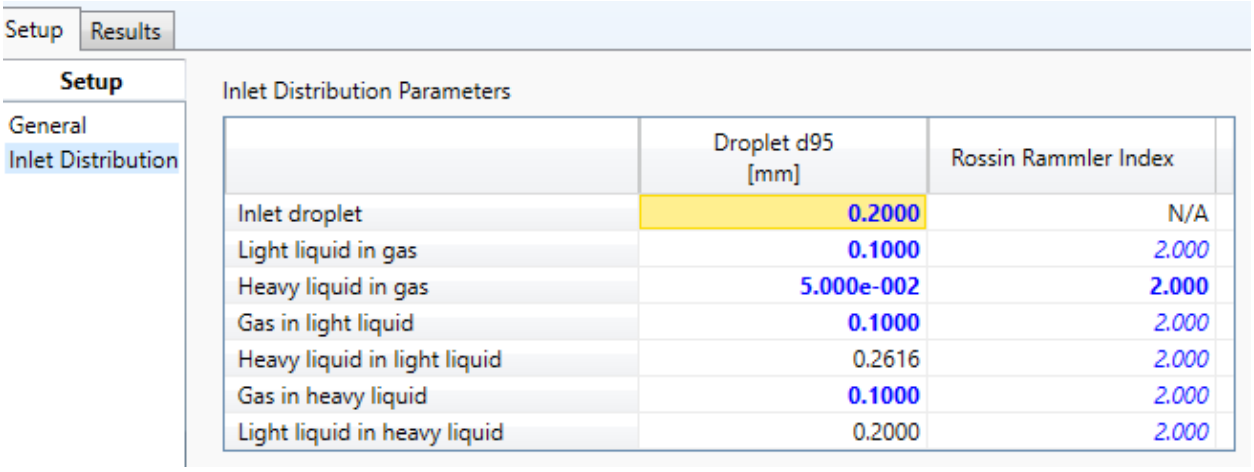

Figure B.6: Basic specification of the dispersions droplets